REPORT DOCUMENTATION PAGE

Form Approved OMB No. 0704-0188

1. REPORT DATE *(DD-MM-YYYY)*	2. REPORT TYPE	3. DATES COVERED *(From – To)*
20-07-2006	Final Report	25 March 2005 - 09-Aug-06

4. TITLE AND SUBTITLE

High Accuracy Multidimensional Parameterized Surrogate Models For Fast Optimization Of Microwave Circuits In The Industry Standard Circuit Simulators

5a. CONTRACT NUMBER
FA8655-05-1-3028

5b. GRANT NUMBER

5c. PROGRAM ELEMENT NUMBER

6. AUTHOR(S)

A. Lamecki, L. Balewski, M. Mrozowski

5d. PROJECT NUMBER

5d. TASK NUMBER

5e. WORK UNIT NUMBER

7. PERFORMING ORGANIZATION NAME(S) AND ADDRESS(ES)
Gdansk University of Technology
Narutowicza 11/12
Gdansk 80-952
Poland

8. PERFORMING ORGANIZATION REPORT NUMBER
N/A

9. SPONSORING/MONITORING AGENCY NAME(S) AND ADDRESS(ES)

EOARD
PSC 821 BOX 14
FPO 09421-0014

10. SPONSOR/MONITOR'S ACRONYM(S)

11. SPONSOR/MONITOR'S REPORT NUMBER(S)
Grant 05-3028

12. DISTRIBUTION/AVAILABILITY STATEMENT

Approved for public release; distribution is unlimited.

13. SUPPLEMENTARY NOTES

14. ABSTRACT

The goal of this project was to advance the techniques for creating multivariate surrogate models of high complexity in order to create full wave models for industry standard circuit simulators (ADS, Microwave Office). The models have the accuracy comparable to full wave simulations but at the same time the computational speed similar to the closed form formulae.

15. SUBJECT TERMS
EOARD, device modeling, rational interpolation

16. SECURITY CLASSIFICATION OF:			17. LIMITATION OF ABSTRACT	18, NUMBER OF PAGES	19a. NAME OF RESPONSIBLE PERSON
a. REPORT	b. ABSTRACT	c. THIS PAGE			GEORGE W YORK, Lt Col, USAF
UNCLAS	UNCLAS	UNCLAS	UL	53	19b. TELEPHONE NUMBER *(Include area code)* +44 (0)20 7514 3154

High accuracy multidimensional parameterized surrogate models for fast optimization of microwave circuits in the industry standard circuit simulators Final report - Grant no FA8655-05-1-3028

Adam Lamecki, Lukasz Balewski
Michal Mrozowski
Gdansk University of Technology, Department of Electronics
80-952, Gdansk, Poland

July 3, 2006

Contents

Chapter 1

Surrogate models

1.1 Introduction

Design of complex microwave systems is carried out using commercial circuit simulators. This is a long process because the design involves the optimization. In microwaves circuits are distributed, so the response depends on the dimensions and topology. The response can be evaluated using either the closed form formulas or full-wave electromagnetic simulators. Full-wave simulators are too slow to be used in an optimization loop, so all circuit simulators employ closed form formulas, or in other words surrogate models. The accuracy and speed of analysis of a simulator relies on fast and accurate surrogate models of microwave discontinuities. Surrogates are used on many stages of a microwave circuit design: from initial design to final optimization and yield analysis. For a microwave designer one of the most import requirements regarding the circuit simulator is the quality and diversity of models library. Recently, new technologies have emerged for low cost millimeter-wave systems based on the system on the chip (SoC) or system on the package (SoP) design philosophies. For instance, SoC employs silicon germanium (SiGe) on either CMOS/BiCMOS-grade Si or highresistivity Si as a replacement for GaAs for some applications. SoP modules integrate different passive components in a multilayer low loss material such as low temperature co-fired ceramic (LTCC) or Liquid Crystal Polymers. Other category are millimeter wave devices made in multilayer MCM-D technology. For these emergent technologies there are no component libraries that can be used with the industry standard circuit simulators such as Agilient's ADS or AWR's Microwave Office. As a result, one has either to apply approximate formulas that are often too inaccurate or resort to a full wave solver in order to design systems components. EM simulations are too computationally intensive to be used in the optimization loop. The design time would be significantly reduced if a designer could use the surrogate parameterized models that could be evaluated at the speed of closed form formulas but having the accuracy comparable to EM simulations. One of the goals of the research in this area is to create a technique that allow one to build a multidimensional parametric model of a component using as few data points as possible.

The development of such a technique was the main motivation for this research. The basic algorithm of surrogate model construction was developed previously and published in two publications [1, 2]. The main assumption is to represent the transfer function of the device being modelled with a multivariate rational function with adaptive support point and model order selection. The technique is the extension of the technique presented in [15] to the multivariate case. The adaptive sampling over whole parameter space was utilized to efficiently select and

limit the number of support points. Detailed description of the technique will be given in next sections.

Given the bacground and the fact that the basic algorithm was already available, the goals of this project was to advance the published technique and prove its viability for microwave circuit design by creating multivariate surrogate models of high complexity of componetns in one of the emerging technologies and ready to use in industry standard circuit simulators (ADS, Microwave Office). The models have the accuracy comparable to full wave simulations but at the same time the computational speed similar to the closed form formulae. As a result one is able to achieve fast optimization of microwave circuits manufactured in the emerging and new technologies. Specifically the following issues were addressed:

- Improvement of stability of the interpolation solvers by replacing multinomials with better conditioned orthogonal polynomials.
- Development of the technique for automated division of the parameter space that will allow on to create different low order models in each subspace
- Development of the technique for merging the submodels into a single model covering a wider parameters range.
- Integration of the software for automated model generation with the industry standard planar structure simulators such as e.g. Sonnet.
- Development of software for automated generation of compiled models that can the used with ADS and Microwave Office
- Demonstration of the suitability of the approach for emerging technologies such as LTCC and LCP, MCM-D by developing models of typical discontinuities or elements e.g. spiral inductors.

1.2 Alternative solutions for model construction

The technique chosen for this effort as a basis for the surrogate model construction has a few alternatives. One popular solution which is applied for surrogate models involves artificial neural networks [3, 4, 5], however the drawbacks of ANN (unknown network topology and long training process) significantly limit their usage in automated model construction. The surrogates can also be created with application of radial basis functions (RBF) [6, 7]. The issue is the selection of best value of unknown shape-parameter of radial functions [8]. On the other hand the approach using RBF's significantly reduces the problems with ill-conditioning. Test carried out by our research group showed however that the RBF's are inefficient in case of complex devices.

Another approach for automatic model creation was presented in [9]. In this algorithm, frequency is handled separately from other physical parameters. The procedure has two stages: at first at selected frequency points multidimensional models are created by expanding the multivariate functions into series of orthogonal multinomials. The expansion coefficients are found by solving a system of interpolatory conditions. On this stage the support points are added in an entirely adaptive way. Next the frequency dependence is added by one-dimensional rational interpolation of the models response. The procedure creates models with good accuracy, but it

is obvious that excluding frequency from the adaptive sampling procedure may result in non-optimal number of support points. Presented results also show that such solution is efficient up to three parameters.

Lehmensiek and Meyer [10, 11, 12] developed techniques based on Thiele-type branched continued fraction representation of a rational function. The algorithms operate by using a univariate adaptive sampling along a selected dimension. In this way, while the support points do not fill the grid completely, they are being added along straight lines passing through multidimensional space. The efficiency of the algorithms was illustrated on two- and three-dimensional models.

Yet another approach uses statistical tools for model construction like Kriging [13] and Design of Experiment (DOE) [14] techniques. Kriging is a special form of interpolation function that employs the correlation between neighboring points to determine the overall function at an arbitrary point. DOE makes a series of tests in which a set of input variables is changed and the experimenter can identify the reasons for changes in the output response. Based on this knowledge one can construct a statistical model if the test structure. Both techniques can be applied to create of simple models with low accuracy and are dedicated to coarse tuning of the design.

1.3 Measures of model quality

In every model construction scheme, the basic question is how to assess the accuracy of the created model. Estimation of the model error is an important issue, because in many cases the accuracy of model limits the range of its applications. There are several criterions of verification of model accuracy. In techniques that involves adaptive sampling, like one described in this report, the basic measure of error is the maximum difference between two different models which are used to select the set of support points. Let us define this error as ε. As described later, the goal of the procedure is to create two different models, in case of which the error ε is below required accuracy ε_0. However the criterion $\varepsilon < \varepsilon_0$ does not guarantee that created model have accuracy as good as ε_0. To estimate the real accuracy of the model, one needs to perform an additional statistical test. The test involves computation of model response on a test set of random points scattered in the model parameter space and compare the results with response of device being modelled. In result one gets a real accuracy of the model, defined in this report as Δ.

Form the data evaluated and randomly selected points one can compute various statistical measures. In this report we use the following simple ones: the maximum real error Δ_{max} and mean real error Δ_{mean}. Both errors can be computed in decibels as $\Delta[\text{dB}] = 20\log(\Delta)$. Such maximum and mean real errors give a good measure of model accuracy. They are however too simple for practical purpose, because they do not provide the information regarding the expected accuracy for a particular set of parameters. Therefore, it appears that it is more meaningful to apply the cumulative distribution function of error Δ to derive the quality measure. In our case we descided to use the error level Δ_{90} that fulfills condition that 90% of points in the test set have an accuracy better than Δ_{90}. As discussed in [16] the error estimate ε has a better correlation with Δ_{90} than with Δ_{mean} or Δ_{max}.

1.4 Technique details

The technique selected for this work creates an interpolant of N variate, real or complex valuated smooth function $S(\underline{X}) = S(x_1, x_2, ..., x_N)$ as a rational function [1]:

$$\widehat{S}(x_1, x_2, ..., x_N) = \frac{A(\underline{X})}{B(\underline{X})} = \frac{A(x_1, x_2, ..., x_N)}{B(x_1, x_2, ..., x_N)} \tag{1.1}$$

where both numerator $A(\underline{X})$ and denominator $B(\underline{X})$ are multinomials (sum of monomials multiplied with scalar coefficients). The complete set of the monomials can be listed as elements of matrix[17]:

Row 1 : 1
Row 2 : $x_1 \;\; x_2 \;\; \ldots \; x_N$
Row 3 : $x_1^2 \;\; x_1x_2 \;\; \ldots \; x_1x_N \;\; x_2^2 \;\; x_2x_3 \ldots x_N^2$
Row 4 : $x_1^3 \;\; x_1^2x_2 \;\; x_1^2x_3 \;\; \ldots \; x_1^2x_N \;\; x_2^3 \;\; x_2^2x_1 \;\; x_2^2x_3 \ldots x_N^3$
...

In the m-th row are written all monomials with sum of powers at each variable equal m-1. With such assumption the multinomials of numerator/denominator can be described with a vector $V = [v_1, v_2, \ldots, v_N]$, where v_i determines maximum allowed power of the i-th variable. For example in case of a three-variate multinomial which order is described with vector $V = [3\ 2\ 2]$ the following monomials are selected:

Row 1 : 1
Row 2 : $x_1 \;\; x_2 \;\; x_3$
Row 3 : $x_1^2 \;\; x_1x_2 \;\; x_1x_3 \;\; x_2^2 \;\; x_2x_3 \; x_3^2$
Row 4 : $x_1^3 \;\; x_1^2x_2 \;\; x_1^2x_3 \;\; x_1x_2^2 \;\; x_2^2x_3 \;\; x_1x_3^2 \;\; x_2x_3^2 \; x_1x_2x_3$

In further investigations it is assumed that both numerator A and denominator B of (1.1) have the same orders, therefore $V_A = V_B = V$.

The unknown coefficients a_i and b_i corresponding to the multinomials of numerator and denominator of 1.1 can be found requiring that equation:

$$A(\underline{X}) - S(\underline{X})B(\underline{X}) = 0 \tag{1.2}$$

is fulfilled in at least $L \geq M_1 + M_2$ support points, where M_1 and M_2 are the numbers of unknown coefficients a_i and b_i. The fitting problem can be transformed to the matrix form:

$$[A \; -B] \begin{bmatrix} a \\ b \end{bmatrix} = 0 \tag{1.3}$$

where a and b are the vectors of unknown coefficients and $[A]_{L\times M_1}, [B]_{L\times M_2}$ are matrices involving the values of the monomials appearing in numerator and denominator of (1.1) as well as the values of the interpolated function at support points.

The problem can be solved applying the total least squares technique, as described in [18]. The total least squares method is suited to problems in which both the coefficient matrix and the right-hand side are not precisely known. It allows one to filter the noise from interpolated

data and improve the quality of resulting solution. The first step is the computation of the QR decomposition of the matrix $C = [A \ -B]$, which results in:

$$\begin{bmatrix} R_{11} & R_{12} \\ 0 & R_{22} \end{bmatrix} \begin{bmatrix} a \\ b \end{bmatrix} = 0 \tag{1.4}$$

where matrix R_{11} has size $(M_1 \times M_1)$, R_{12} has size $(M_1 \times M_2)$ and R_{22} is $((L - M_1 + 1) \times M_2)$ matrix. The R_{22} matrix is affected by the noise. The equation (1.4) can be written as two separate equations:

$$[R_{11}]a = -[R_{12}]b \tag{1.5}$$

$$[R_{22}]b = 0 \tag{1.6}$$

Computing the singular value decomposition (SVD) of R_{22} one obtains:

$$[U][\Sigma][V]b = 0 \tag{1.7}$$

where matrix V is size $(M_2 \times M_2)$. The solution of the problem in TLS sense is proportional to the last column of the matrix V, therefore is assumed that $b = [V]_{M_2}$.

1.4.1 Condition number improvement

Condition number in least squares measures the sensitivity of the solution of a system of linear equations to errors in the data. The value of condition number allows one to decide if the solution of the least squares is reliable and accurate. Namely a value of the conditioning number near 1 indicates well-conditioned least squares problem. The conditioning number is computed as a ratio of the largest singular value of matrix that forms a least squares problem to the smallest one.

A major issue of rational interpolation is a poor conditioning of equation system. In order to cope with this this problem two techniques are recommended:

- Mapping each of variables to a line segment <-1,1>
- Substitution of simple monomials with orthogonal Tchebychev polynomials

The first technique is linear mapping of model's domain to the multidimensional box with side of line segment. The mapping of a i-th variable x_i is expressed by formula:

$$x_{i,m} = 2\frac{(x_i - x_{0,i})}{\Delta x_i} \tag{1.8}$$

where $x_{i,m}$ is a mapped variable, $x_{0,i}$ denotes center point of the parameter range and Δx_i denotes the width of the parameter range.

To improve the conditioning of the interpolation problem the regular elements x_i^n composing the monomials are replaced with Tchebychev polynomials $T_n(x_i)$, that are orthogonal on line segment $< -1, 1 >$. Tchebychev polynomials can be computed using recurrence formula:

$$\begin{aligned} T_1(x) &= 1 \\ T_2(x) &= x \\ T_3(x) &= 2x - 1 \\ T_4(x) &= 4x^2 - 3x \\ &\vdots \quad \vdots \\ T_{n+1}(x) &= 2x \cdot T_n(x) - T_{n-1}(x) \end{aligned}$$

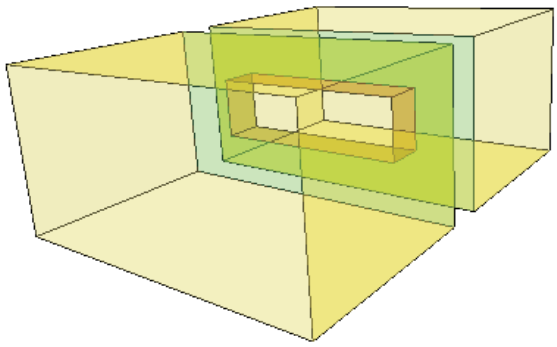

Figure 1.1: Iris in rectangular waveguide

Table 1.1: Range of parameters of rectangular iris model

Parameter	Range
frequency f	11.855GHz - 18.02GHz
width a	6.32mm - 15.8mm
height b	4.74mm - 7.899mm
thickness d	0.2mm - 2mm

As an result, the set of monomials is transformed into form:

Row 1 : 1
Row 2 : $T_1(x_1)\ \ T_1(x_2)\ \ \ldots\ \ T_1(x_N)$
Row 3 : $T_2(x_1)\ \ T_1(x_1)T_1(x_2)\ \ \ldots\ \ T_1(x_1)T_1(x_N)\ \ T_2(x_2)\ \ T_1(x_2)T_1(x_3)\ldots T_2(x_N)$
Row 4 : $T_3(x_1)\ \ T_2(x_1)T_1(x_2)\ \ T_2(x_1)T_1(x_3)\ \ \ldots\ \ T_2(x_1)T_1(x_N)\ \ T_3(x_2)\ \ T_2(x_2)T_1(x_1)$
$T_2(x_2)T_1(x_3)\ldots T_3(x_N)$
...

Example. The improvement of the conditioning of the problem in case of a rational model of scattering parameter S_{11} of an iris (figure 1.1) in rectangular waveguide WR62 is presented. The selection of the structure is motivated by fast computation of electromagnetic response with a mode-matching technique and complex (resonant) response (figure 1.2). The model involves four parameters: frequency, iris width, height and thickness. The range of parameters is presented in table 1.1. The data were interpolated with orthogonal and non-orthogonal functions, for different rectangular grid resolution D and with or without mapping of model domain. The results of such conditioning test are presented in tables 1.2 and 1.3. It can be seen that the proposed approach provides a significant reduction of the condition number, which assures better reliability of constructed models.

1.4.2 Selection of support points

Optimal support point selection is an essential issue of every interpolation scheme. It is especially important in case of modelling of multivariate functions where the number of support

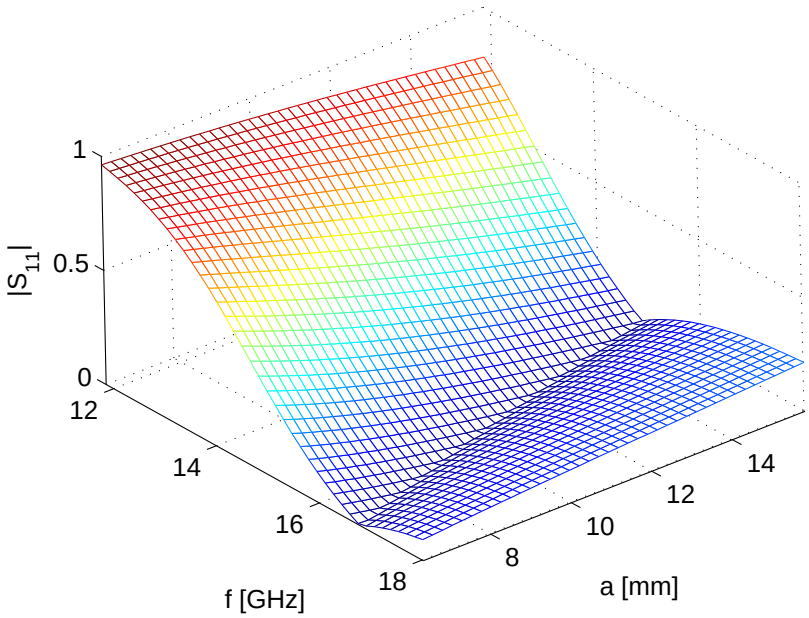

Figure 1.2: Sample S_{11}(f,a) response of iris in WR62 rectangular waveguide with iris height $b = 6.32$mm and iris thickness $d = 1.1$mm.

Table 1.2: Condition number computed in waveguide iris case for rectangular grid with divisions $D = 4$ and different polynomials

Model order V	Space, Polynomials		
	Non-mapped, Regular	Mapped, Regular	Mapped, Tchebychev
[2 2 2 2]	6692.3	186.3	136.5
[3 3 3 3]	508300	1489.5	1139.1

Table 1.3: Condition number computed in waveguide iris case for rectangular grid with divisions $D = 6$ and different polynomials

Model order V	Space, Polynomials		
	Non-mapped, Regular	Mapped, Regular	Mapped, Tchebychev
[2 2 2 2]	7428	194.1	142.7
[3 3 3 3]	275350	1037	746.4

points can be enormous. Since each point corresponds to one electromagnetic simulation of device being modelled, it is obvious that a minimization of samples number is critical. The simplest choice of dense multidimensional rectangular grid is not optimal, due to fast growth of number of samples with increase of grid resolution and number of model parameters (see table 1.4).

In proposed technique an adaptive sampling technique called also *reflective extrapolation* is used [9]. The idea of adaptive sampling is to create two different models ($\hat{S}_1(\underline{X})$ and $\hat{S}_2(\underline{X})$) of the modelled function and place additional samples at the points of biggest mismatch between both models $\varepsilon = \|\hat{S}_2(\underline{X}) - \hat{S}_1(\underline{X})\|$. Such a procedure, reiterated, leads to model quality

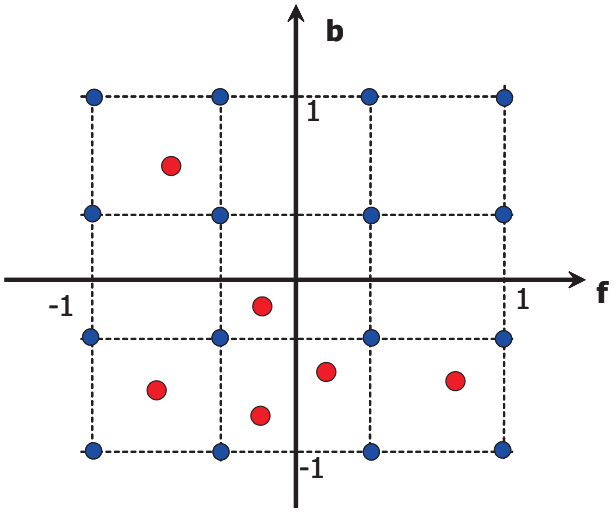

Figure 1.3: Two dimensional example of support points selection - added points are placed in non-regular manner over the parameter space.

improvement and minimizes the number of samples used, which is especially advisable if the models are based on results of electromagnetic simulations. The procedure is reiterated until the mismatch ε between low and high order model drops below required tolerance ε_0.

An important issue is a search procedure of the point of biggest mismatch. This problem corresponds to problem of search of maximum of multivariate function over a multi-dimensional box and especially in the case of high number of model parameters this issue has to be solved efficiently. To deal with this problem a genetic optimization procedure was applied. The advantage of genetic optimization is that it allows to find a global, not local, minimum of the function. The search is performed over the whole parameter space of the model, like presented in figure 1.3, and the technique gives better results than approaches in which the parameter space is searched with structured pattern (like grids).

It has to be noted that since a goal of adaptive sampling is the minimization of error $\varepsilon = \|\hat{S}_2(\underline{X}) - \hat{S}_1(\underline{X})\|$, the overall accuracy of resulting models can be worse than ε_0. Such

Table 1.4: Number of support points needed for N-dimensional rectangular grid with resolution D

Variables	Divisions					
	1	2	3	4	5	6
1	1	2	3	4	5	6
2	2	4	9	16	25	36
3	3	8	27	64	125	216
4	4	16	81	256	725	2196
5	5	32	243	1024	3125	7776
6	6	64	729	4049	15625	46656
7	7	128	2187	16384	78125	279936

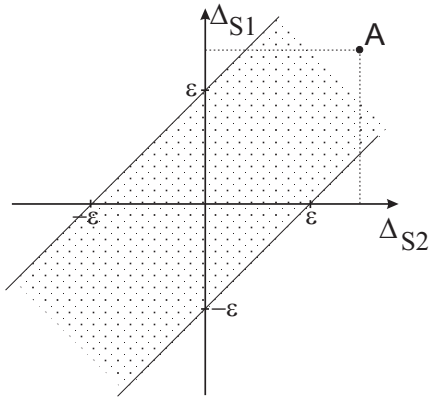

Figure 1.4: Range of model error for mismatch between models equal error ε.

situation is possible when both models converge to the function which slightly differs from electromagnetic response. Let Δ_{S1} and Δ_{S2} represent the real error of models $\hat{S}_1(\underline{X})$ and $\hat{S}_2(\underline{X})$ related to electromagnetic response. Assume that the maximum acceptable error between both models is ε_0. In this case the possible values of model error Δ_{S1} and Δ_{S2} are illustrated in figure 1.4 (dotted area). For example, in case of the point *A*, the real error Δ_{S1}, Δ_{S2} of both models is higher than ε, however the relative error between both models is below ε because the real errors of both models have the same signs.

During adaptive sampling process a clustering of support points can occur, i.e. the subsequent support points are added in the same location. The interpolation problem is then expanded with the same points which do not give any extra information about the device response, but make the problem bigger and harder to solve. Such situation should be eliminated, therefore if algorithm detects such behavior, the parameter space is divided into 2^N smaller subspaces (each dimension is divided to half) and the locations of biggest mismatch between models in those 2^N subspaces is found. The set of points is appended to the data set and the adaptive sampling continues.

Implementation of described adaptive sampling makes it possible to detect if the interpolation problem is ill-conditioned. The models obtained as a solution of ill-conditioned system do not match each other and in result error between both models is large (namely $\varepsilon > 1$). If such situation occurs on the initial stage of model construction, when the number of support points is small, the solution is to add more points to the system and improve the conditioning. Another case when the ill-conditioning of the system occurs is if the order of the models become to high. In this case the scheme of parameter space division can be applied to construct the model, as described in section 1.4.4.

Example. To show the benefits of adaptive sampling over a uniform rectangular grid a comparison of mentioned techniques is presented. The model order was constant and selected as $V_{S1} = [2\ 2\ 2\ 2]$. Model accuracy for different density *D* of grid is presented in table 1.5, figure 1.5 shows the histograms of the model error. To compute the histograms a iris response on 10000 random data points was computed in electromagnetic solver and compared with model response. The error was computed as direct difference between model and simulation response $\Delta = \|S(\underline{X}) - \widehat{S}(\underline{X})\|$. Figure 1.5 also presents a cumulative distribution function of the error computed on the same 10000 points, that shows which percent of samples has accuracy equal

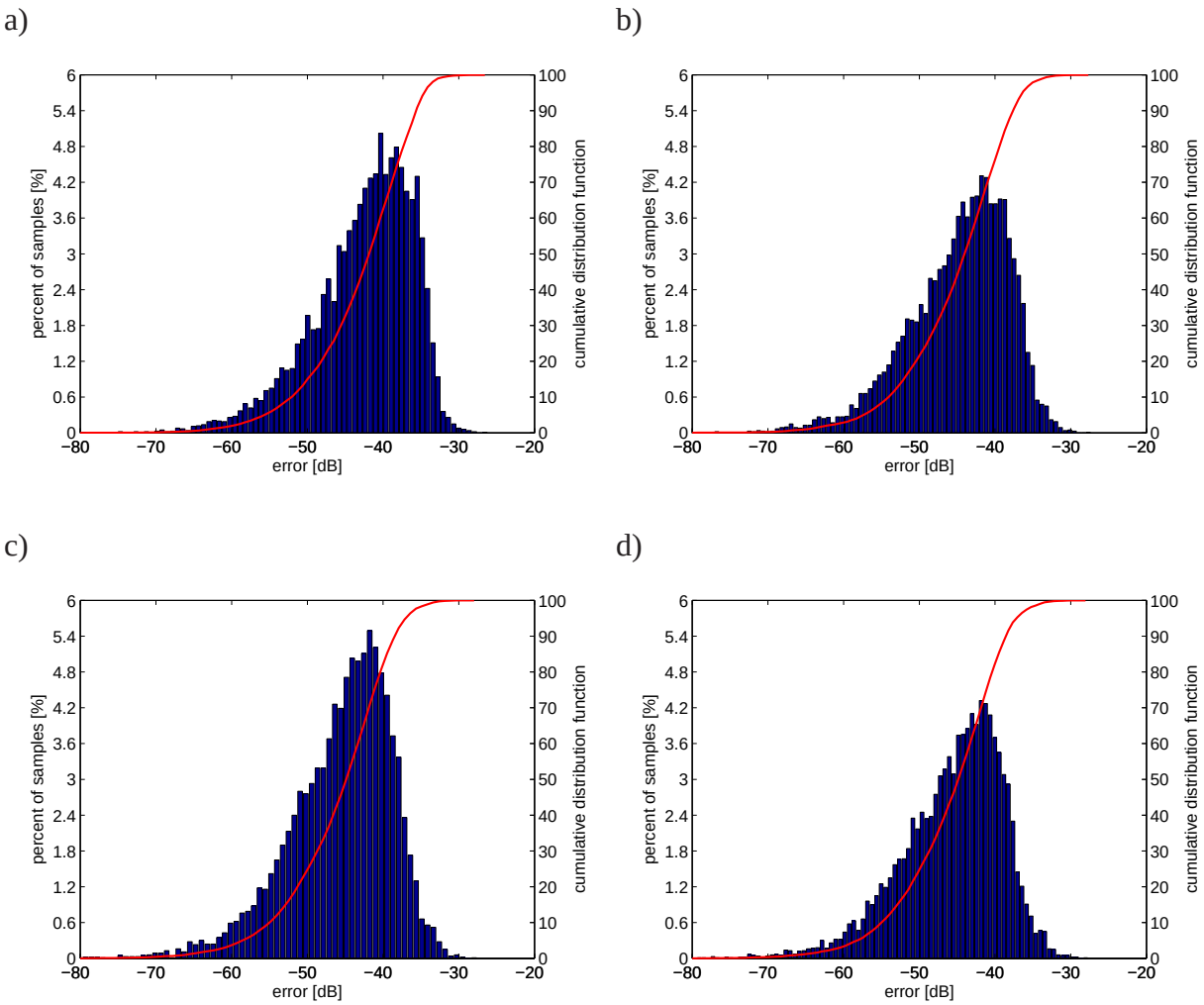

Figure 1.5: Histogram and cumulative distribution function of model error for different grid density: a) $D = 4$, b) $D = 5$, c) $D = 6$, d) $D = 7$

Table 1.5: Model accuracy vs. density of rectangular grid

D	M	Δ_{max} [dB]	Δ_{mean} [dB]
4	256	-26.54	-40.66
5	625	-27.67	-42.71
6	1296	-27.97	-43.46
7	2401	-28.03	-43.56

or better than given error.

As expected, the more dense is the rectangular grid, the better accuracy of the computed model can be observed. However, comparing the improvement of the model accuracy to the number of support points, it have to be noted that increase of the grid's density is not an efficient way to improve the model quality.

To compare, the same model was created with application of adaptive sampling technique. An initial sparse grid resolution was $D = 3$ (the grid had only 81 points). The initial data set

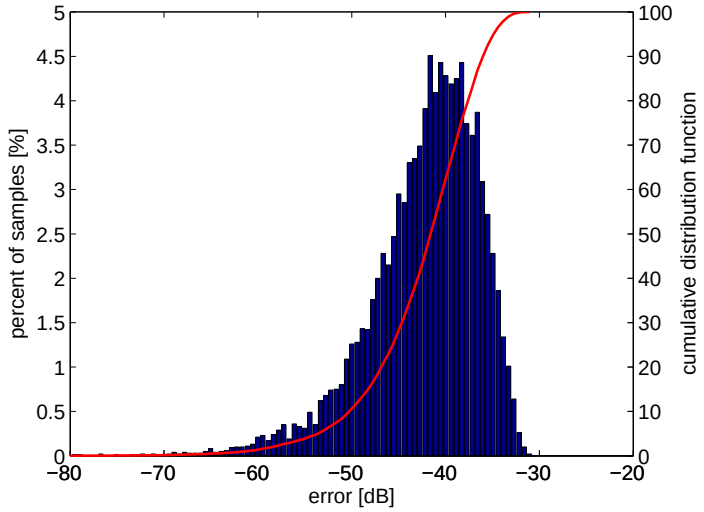

Figure 1.6: Histogram and cumulative distribution function of model error with adaptive sampling technique

Table 1.6: Model accuracy using adaptive sampling technique

M	Δ_{max} [dB]	Δ_{mean} [dB]
100	-28.15	-37.85
125	-29.55	-39.41
150	-28.49	-39.91
175	-29.95	-40.44
250	-29.51	-40.50

was appended with application of adaptive sampling. The model accuracy vs. number of points added is depicted in table 1.6. It can be observed that a addition of data set of 19 points gives a smaller maximum model error than a rectangular grid consisting of 2401 points, and further application of adaptive sampling improves the model accuracy. The adaptive model constructed on 175 data points has a similar mean error as the model created on a rectangular grid of 256 data points and maximum error is reduced by half. However, if the adaptive sampling procedure continues with the same model orders, supplementing of the data set improves the model accuracy marginally.

QR-update. The described procedure requires one to update both models each time a support point is added. It means, that one have to recompute the TLS solution of interpolation problem in every iteration. To reduce the numeric cost of such operation an *QR*-update procedure can be used [19]. Assume that matrix C has a factorization $C = Q \cdot R$, where Q is orthogonal and R is upper triangular. Addition of a single support point appends a vector w^T to the matrix C. As an result one obtains updated matrix:

$$\hat{C} = \begin{bmatrix} w^T \\ C \end{bmatrix} \tag{1.9}$$

Additionally, one can notice that:

$$diag(1, Q^T) \cdot \hat{C} = \begin{bmatrix} w^T \\ R \end{bmatrix} = H \tag{1.10}$$

where H is an upper Hessenberg matrix. It is possible to apply a set of n subsequent Givens rotations that transform H to upper triangular form:

$$R_1 = J_n^T \; J_{n-1}^T \; \ldots \; J_1 \tag{1.11}$$

Once the Givens rotations are known, the matrix Q_1 can be computed as:

$$Q_1 = diag(1, Q) \; J_1 \; J_2 \; \ldots \; J_n \tag{1.12}$$

Matrices R_1 and Q_1 form a QR factorization of matrix $\hat{C} = Q_1 \cdot R_1$.

The full QR factorization form scratch is algorithm of complexity $O(N^3)$, while update of the existing Q and R matrices is $O(N^2)$ algorithm.

1.4.3 Order selection

The application of adaptive sampling using constant model orders is not sufficient to automated model construction. The key element in investigated interpolation procedure is a development of efficient technique of model order selection.

The adaptive sampling procedure uses two different models which are iteratively compared to each other. The models $\hat{S}_1$ and $\hat{S}_2$ are described with two vectors V_{S1} and V_{S2}. To ensure the best performance of the technique the initial models have low complexity and an algorithm of automated order selection is applied. The minimal model order considered is $V_{S1}(1:N) = 2$ and is assumed that model $\hat{S}_2$ has a higher order allowed than model $\hat{S}_1$.

Orders of initial models

The initial models should be of a similar order. In fact, the more both models differ each other, the more data points is needed the algorithm to converge. However it marginally influence the accuracy of final models, because the lower order model limits the accuracy.

To prove this a models of the same rectangular iris as described before were constructed applying adaptive sampling with different pairs of models order selected:

- $V_{S1} = [2\ 2\ 2\ 2]$, $V_{S2} = [3\ 2\ 2\ 2]$
- $V_{S1} = [2\ 2\ 2\ 2]$, $V_{S2} = [3\ 3\ 2\ 2]$
- $V_{S1} = [2\ 2\ 2\ 2]$, $V_{S2} = [3\ 3\ 3\ 2]$

The initial data set was appended with 100 points by adaptive sampling. Figure 1.7 shows the histogram and cumulative distribution function of error of models low and high order. It can be seen that the accuracy is mainly function of model order. In practical computations the more both models differ each other, the more support points is needed to reach the required accuracy ε_0. To obtain the best performance (accuracy comparing to number of support points) the smallest difference between both models is required. We propose to use $V_{S1}(1:N) = [2\ 2\ \ldots 2]$ and $V_{S2}(1:N) = [3\ 2\ \ldots 2]$ and improve the accuracy with efficient adaptive model order selection.

a1) V = [2 2 2 2]

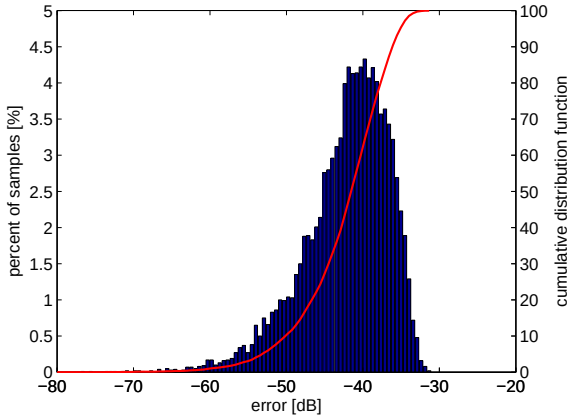

a2) V = [3 2 2 2]

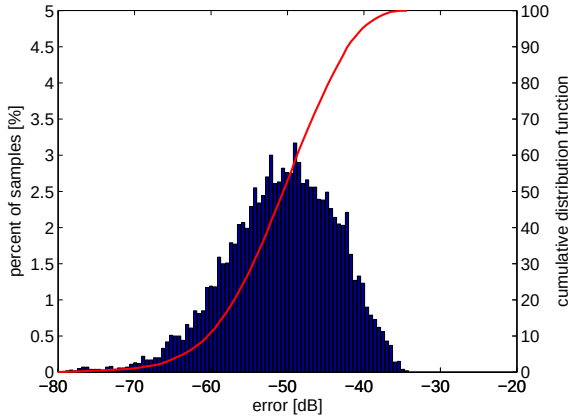

b1) V = [2 2 2 2]

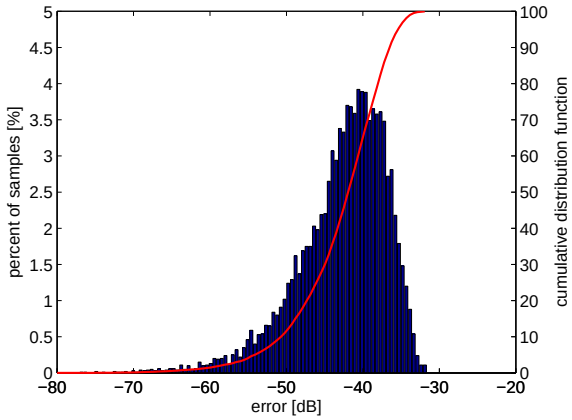

b2) V = [3 3 2 2]

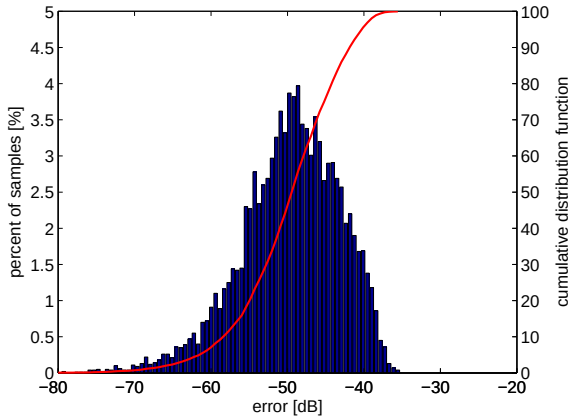

c1) V = [2 2 2 2]

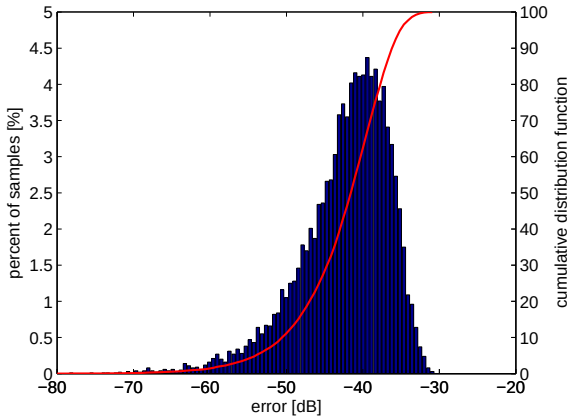

c2) V = [3 3 3 2]

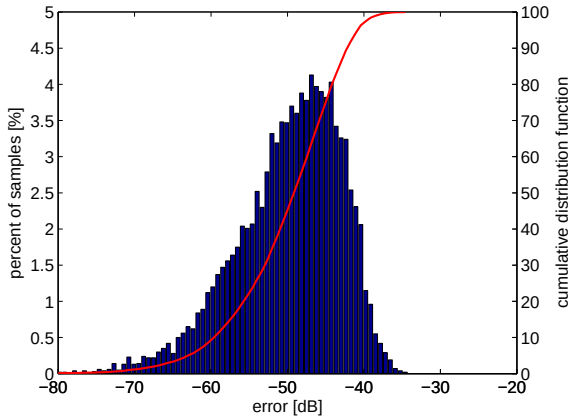

Figure 1.7: Histograms and cumulative distribution function of model error for different pairs of models used in the adaptive sampling

Adaptive model order selection

The whole procedure starts with a sparse rectangular grid of support points and low order models. The technique monitors the error between two models created in an iterative way with

Table 1.7: Model accuracy and number of support points vs. difference between models.

Model	Δ_{max} [dB]	Δ_{mean} [dB]
$V_{S1} = [2\ 2\ 2\ 2]$	-31.32	-40.70
$V_{S2} = [3\ 2\ 2\ 2]$	-34.37	-48.15
$V_{S1} = [2\ 2\ 2\ 2]$	-31.90	-41.12
$V_{S2} = [3\ 3\ 2\ 2]$	-35.56	-47.54
$V_{S1} = [2\ 2\ 2\ 2]$	-30.91	-40.76
$V_{S2} = [3\ 3\ 3\ 2]$	-34.60	-47.58

adaptive sampling. The behavior of the error is a basic indicator if the model order should be increased. It was presented previously that subsequent addition of support points improves the model quality until the stagnation phase. The basic method to detect this is to observe the number of iterations without error improvement. In our tests we decided that number from range 2^{N-1} up to 2^N iterations without improvement is a good indicator that the current order (described by vector V) is too low and has to be increased. To make the algorithm more efficient only these elements of vector V which change make the biggest reduction of error ε are raised.

To show the efficiency of the technique the waveguide iris model was created. The initial grid with $D = 3$ was computed and subsequent data points were added with adaptive sampling. The set of 59 points was added until the stagnation was detected. The model order was increased and the next 9 points was added until the difference between model decreased below the required level 0.003. The mean error of created model is -49.5dB and maximum error is -33.02dB. The histogram of model error and cumulative distribution function are depicted on figure 1.8. It can be seen that proposed technique allowed to generate the model in complete automated way with good accuracy.

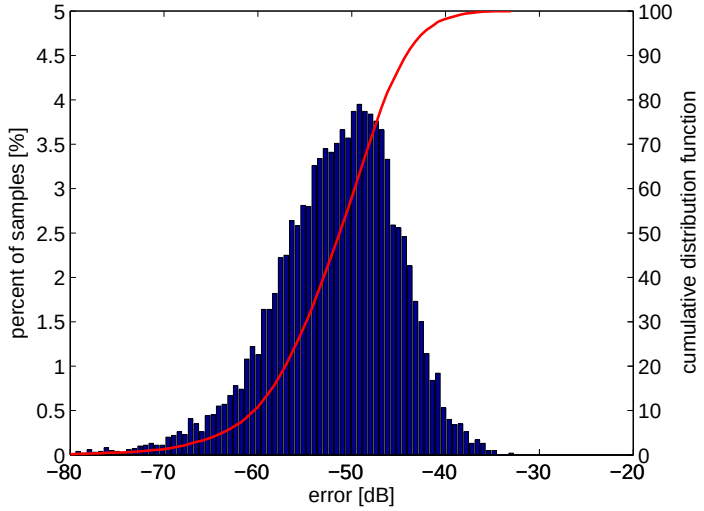

Figure 1.8: Histogram and cumulative distribution function of model error with adaptive sampling technique and automated order selection

In some cases such procedure is not sufficient to construct a single model of device's response due the ill-conditioning of the interpolation problem. It may occur if the model orders are too high and in this case the technique of parameter space division is applied.

1.4.4 Division of parameter space

Division of parameter space is essential if the response of complex device is modelled (for example has several resonances) and/or superb accuracy is requested. In such cases it might be impossible to construct a single rational model which covers whole parameter space and assures desirable accuracy. To overcome the problem an automated technique of parameter space division was developed.

The most important issue is to develop criteria of space division. In proposed technique two cases can cause the division of parameter space during the adaptive sampling procedure:

- The size of the problem becomes too big to be efficiently solved
- Further increasing of model orders leads to ill-conditioned interpolation problem

If one of the conditions if fulfilled, the adaptive sampling stops and the variance analysis for each the model parameters is performed. The smaller is variance of distribution of samples connected with parameter x_i the more data points are concentrated around mean value of x_i. High concentration of data points in some area suggests that in that place/dimension the model is poor, therefore that dimension is selected to be divided. Algorithm creates two smaller subspaces with division of range of selected parameter into halves. Such procedure is implemented as recursive one.

To illustrate the proposed algorithm a simple case of two-variate function $S(x_1, x_2)$ is presented on figure 1.9. Figure shows that initial parameter space was divided into three non-overlaping smaller subspaces. The generalization to N-dimensions is straightforward.

To show the robustness of the technique, it was used to create very accurate model of waveguide iris. The required accuracy of model was established as $\varepsilon_0 = 0.001$ (-60dB). The procedure started from sparse grid of 81 support points and adaptive sampling and order selection reduced the error level to value 0.002. Further increasing of models order resulted in ill-conditioning of the problem. It is worth to notice, that it would be the maximum accuracy possible to obtain without application of parameter space division.

To meet requested accuracy the initial parameter space shown in table 1.1 was sequentially divided into three subspaces, presented in table 1.8. At first the range of width of iris was divided, then in one of the subspaces the frequency range was divided. For each subspace an independent model of device response was created. The histogram and cumulative distribution function of model error are presented on figure 1.10. 90% of samples have accuracy better than -50dB. The mean error of model is -55.97dB and maximum error drops to -38.55dB. The total number of support points is M=460.

1.4.5 Merging submodels

The main disadvantage of space division is a non-smooth response of the models at point of connection of their domains. Since it is impossible to impose the continuity conditions directly into model computation algorithm, this problem has to be solved separately during computation

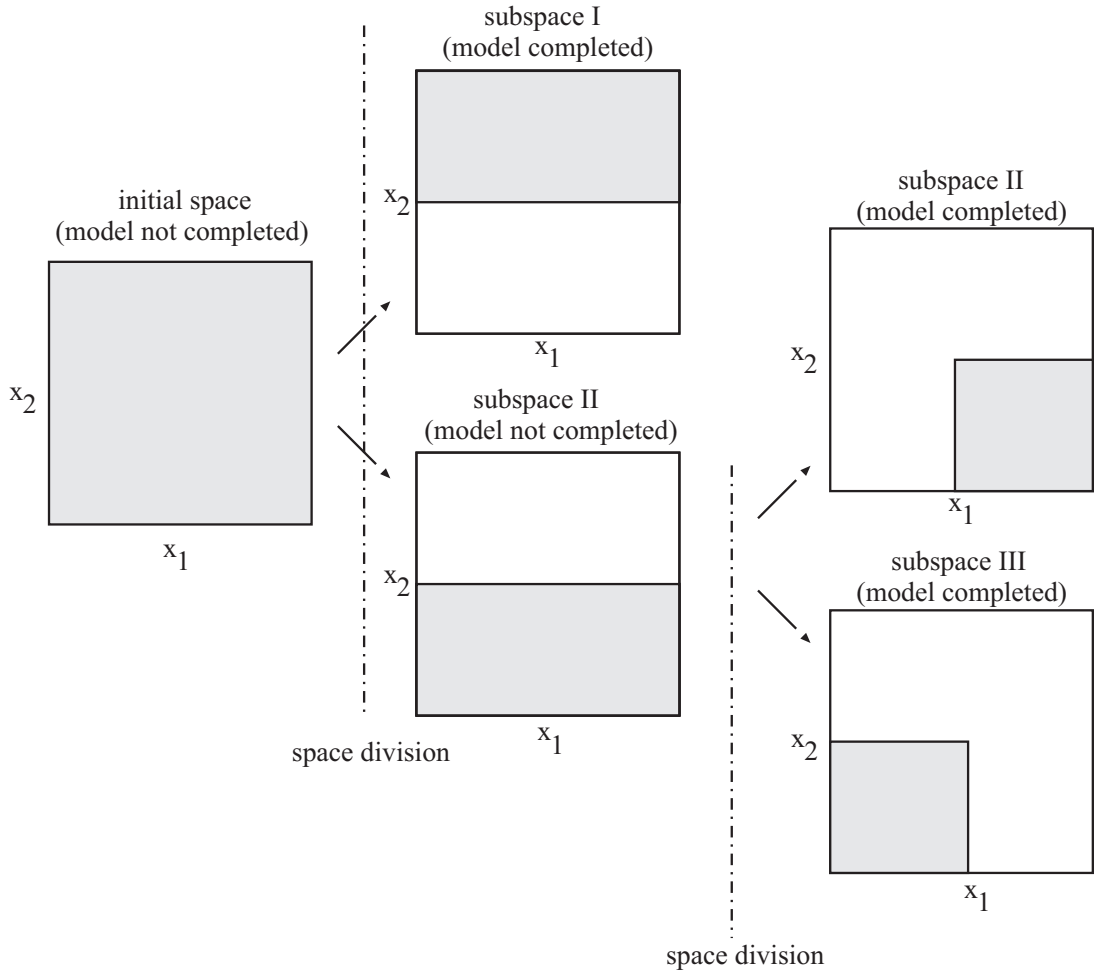

Figure 1.9: Sample space division in two-dimensional case $S(x_1, x_2)$.

of the model response. The problem is illustrated in figure 1.11, that shows a plot of S_{11} parameter computed as an response of two models that cover this frequency range. The discontinuity of the response can be observed directly at the point where the parameter space was divided.

In most of model applications the presence of response discontinuity is not an important issue. It is possible to perform a successful design using such non-smooth model even when

Table 1.8: Parameter ranges for three subspaces created with automated parameter division scheme

Parameter	Model I	Model II	Model III
frequency	11.855GHz - 18.02GHz	11.855GHz - 14.9375GHz	14.9375GHz - 18.02GHz
width	6.32mm - 11.06mm	11.06mm - 15.8mm	11.06mm - 15.8mm
height	4.74mm - 7.899mm	4.74mm - 7.899mm	4.74mm - 7.899mm
thickness	0.2mm - 2mm	0.2mm - 2mm	0.2mm - 2mm

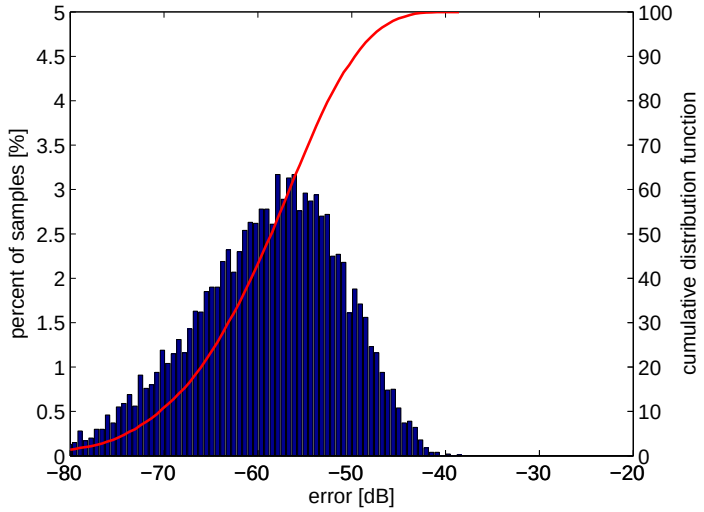

Figure 1.10: Histogram and cumulative distribution function of model error in case of automated space division used

the optimization of the structure is involved. However, if one needs a smooth response in whole parameter space, it is possible to compensate the discontinuity. One can use a cubic spline interpolation procedures in the area of model connection, as presented in figure 1.11. In this approach, a model response in area of the model connection is computed from cubic spline interpolation, generated from six points located near to the model connection (3 points from each model are taken into account). Application of cubic splines gives as result smooth response with continuous first derivative of the response. Additionally it is fast and easy to implement.

1.4.6 Models of multi-port components

The technique described in the previous paragraphs can be used to construct a model of single scattering parameter versus frequency and structure dimensions. In practice, an engineer uses multi-port components, which are described with scattering matrix that contains several scattering parameters. To create a complete model of such a device all the elements of the scattering matrix should be modelled in an independent way. However, to speed up this process significantly, the successive model can utilize the results of electromagnetic simulations that were already performed. In such a case, at the beginning of model creation the sparse grid is used to create the model of first scattering parameter with adaptive sampling and order selection. At this stage the results of simulations of all scattering parameters are stored. Once the procedure converges, all the stored data points can be used to start the generation of model subsequent scattering parameter. Each time the modelling of subsequent scattering parameter is started, a test for initial model orders can be performed. The test generates several models with increasing orders and evaluates the biggest mismatch between chosen pairs. The orders of a model pair with the smallest mismatch are used as initial orders for adaptive model construction scheme.

The presented formulation of multi-port device model construction can also be used to create models of multi-mode devices, as discussed in [2].

1.4.7 Complete algorithm - flow chart

The flow chart of proposed algorithm is presented on figure 1.12. In the main loop an adaptive sampling of the parameter space is performed. In this loop the condition for increasing of model orders is checked and detection of ill-conditioning is performed.

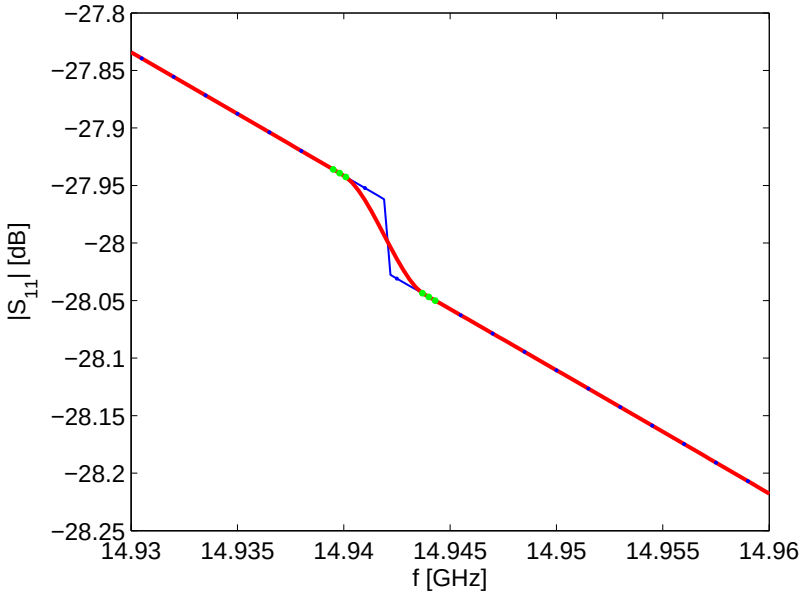

Figure 1.11: Results of proposed technique of model's response discontinuity compensation: — Non-smooth model response, — spline compensated model response, ··· points used for spline computation

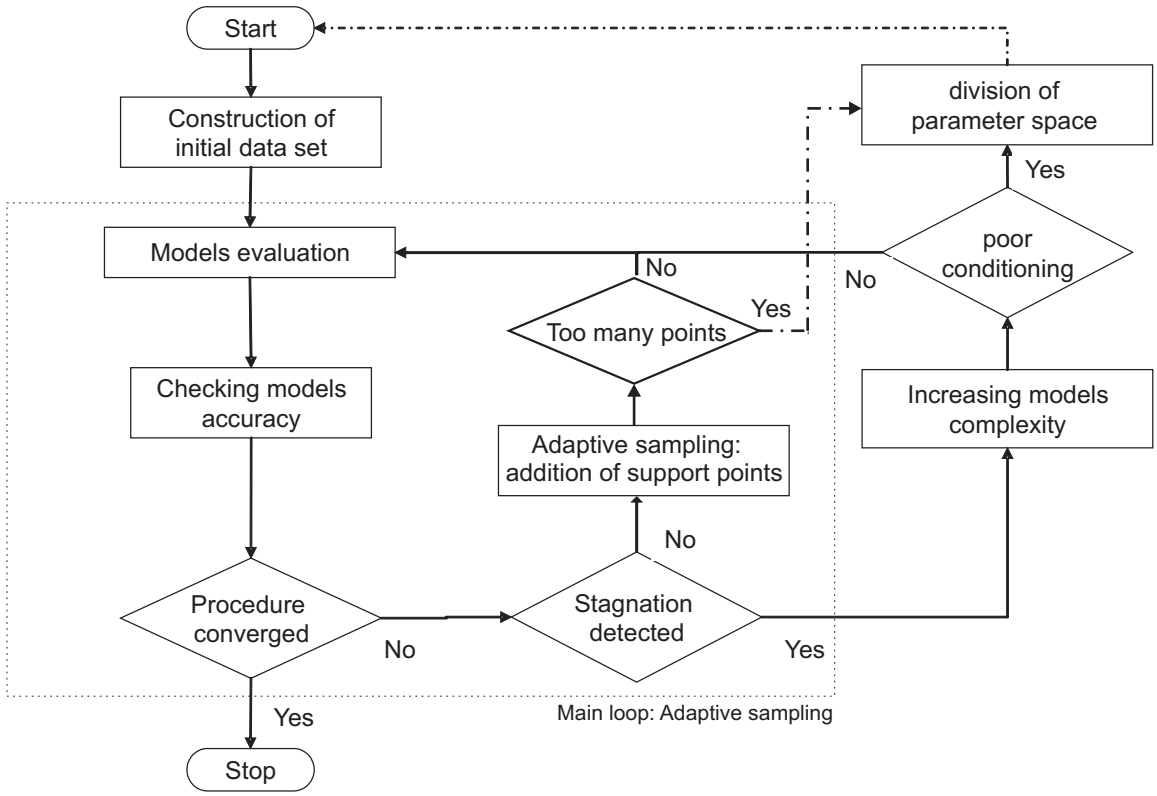

Figure 1.12: Flow chart of complete algorithm

1.5 State-of-the-art examples

The illustrate the flexibility of proposed technique models of two very complex planar devices were created. In both cases the structures were simulated using a commercial electromagnetic solver Momentum. These examples, along with the waveguide iris model presented in section 1.4.4, shows that with proposed technique it is possible to create a surrogates of complex microwave devices.

1.5.1 Spiral inductor in SiGe BiCMOS technology

Structure overview of an octagonal spiral inductor is presented on figure 1.14. Figure 1.15 shows a three dimensional view of the structure along with current visualization on the surface of the inductor. The inductor consists of 2.5 loop spiral with an uniform strip at the top layer and metal bridge at lower layer. The structure is described with three geometric parameters: strip width w, gap width s and inner spiral radius R. The model of such structure was computed in frequency range from DC to 10GHz. Three scattering parameters were modelled: s_{11}, s_{21} and s_{22}. A range of model parameters is presented in table 1.9. Selected parameter range corresponds to approximate inductor die area range from $150\mu m \times 150\mu m$ up to $470\mu m \times 470\mu m$. The required tolerance was set as ε=0.001, and the procedure needed 285 support points to build the models. The time of single analysis was from 3 to 5 minutes on a 1.5GHz PC and depends of structure size.

Then a set of 500 randomly distributed data points in the model domain was generated. The set was used to verify the accuracy of the model. The mean error computed over the set was -67.3dB, while maximum error reaches -55dB. Figure 1.16 shows a histogram and cumulative distribution function of the model error of S_{11}. It can be seen, that 90% of samples has an error below -63dB. Additionally the histogram and cumulative distribution function of error of Q

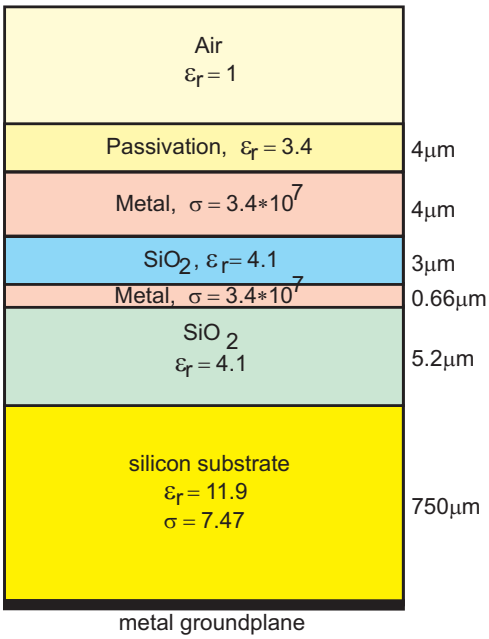

Figure 1.13: Silicon substrate as simulated in ADS Momentum

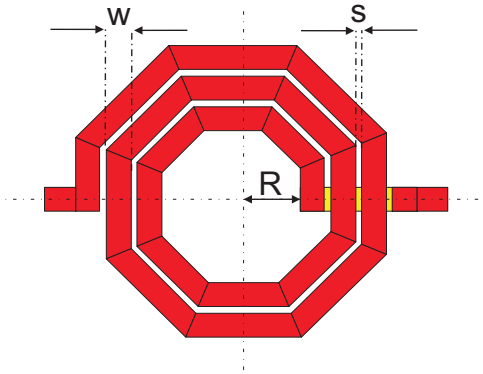

Figure 1.14: Structure and dimensions of modelled octagonal inductor.

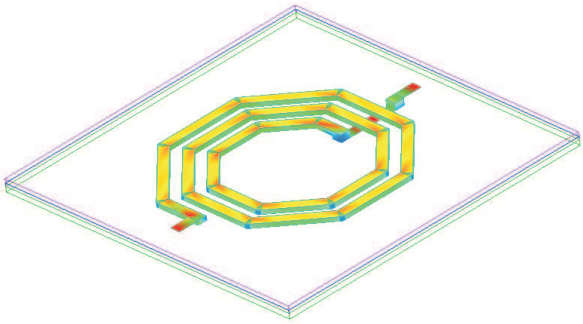

Figure 1.15: Three dimensional field visualization of modelled inductor.

factor computed from model response is presented in Fig.1.17. Despite good accuracy of the models of scattering parameters, the error of extracted Q factor can be high. However the high error appears very near of the inductor resonance (scattering matrix is close to unitary matrix) and in this point the parasitic capacitance of the inductor dominates. In fact this point of inductor operation is out of applications.

Table 1.9: Range of input parameters of spiral inductor model

Parameter	Range
frequency (f)	0GHz - 10GHz
strip width (w)	$10\mu m$ - $25\mu m$
gap width (s)	$5\mu m$ - $20\mu m$
inner radius (R)	$30\mu m$ - $100\mu m$

1.5.2 Interdigitated capacitor in MCM-D technology

A next example is an interdigital capacitor made in MCM-D technology. Thin film MCM-D technology has many advantages over the traditional hybrid technologies. It assures high precision components, repeatability of manufacturing complex microwave structures and integration of analog and digital circuits.

A layout of an interdigitated capacitor made in MCM-D technology is shown on figure 1.18. A model of six variables (frequency and five geometric dimensions) was created. The ranges of the model parameters are presented in table 1.10. The substrate parameters are as follows: thickness $45\mu m$, dielectric permittivity $\varepsilon_r = 2.65$, dielectric losses $\tan\delta = 0.002$, metal thickness $3\mu m$, metal conductivity $\delta = 4.525 \cdot 10^7 \frac{S}{m^2}$ (gold).

The requested modelling error was ε =0.001=-60dB. The procedure started using a sparse grid with D=3 (729 support points) and initial orders $V = [2\ 2\ 2\ 2\ 2\ 2]$. Adding of 1402 data points with increasing of orders to $V = [3\ 4\ 3\ 4\ 4\ 4]$ gives the mismatch between both models below the requested 0.001. To verify the model accuracy a set of 3000 randomly distributed data points were computed using an electromagnetic simulator and compared with model response.

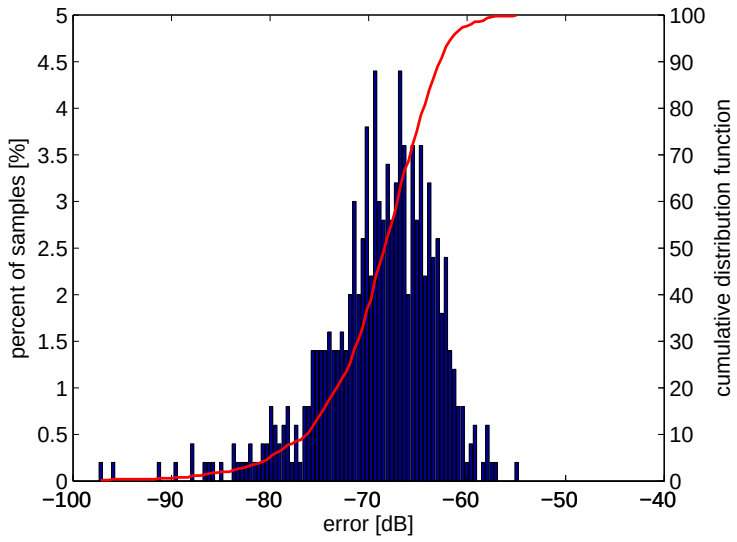

Figure 1.16: Histogram and cumulative distribution function of S_{11} model of octagonal inductor.

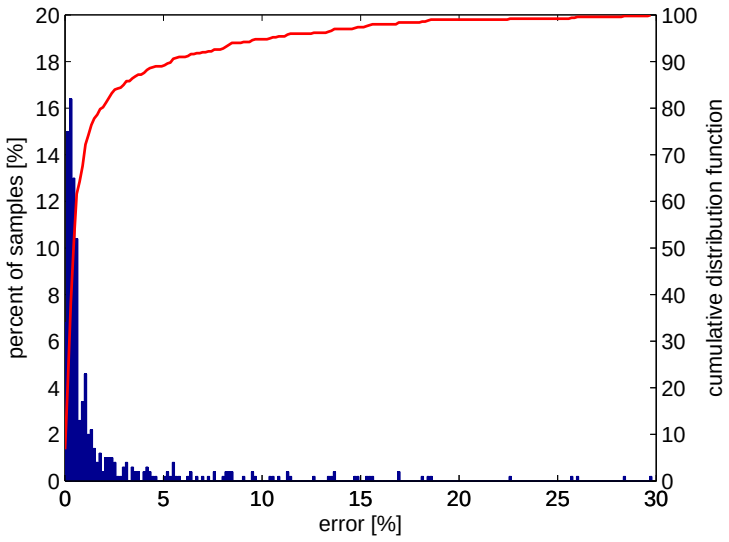

Figure 1.17: Histogram and cumulative distribution function of Q-factor error of rational model of octagonal inductor.

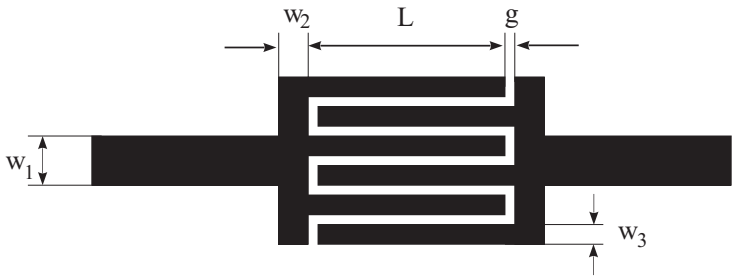

Figure 1.18: Layout of interdigitated capacitor

Table 1.10: Range of input parameters of interdigitated capacitor model

Parameter	Range
frequency (f)	10GHz - 90GHz
input line width (w_1)	$50\mu m$ - $150\mu m$
cap. line width (w_2)	$10\mu m$ - $25\mu m$
finger length (L)	$100\mu m$ - $250\mu m$
finger line width ($w3$)	$10\mu m$ - $20\mu m$
gap width (g)	$10\mu m$ - $25\mu m$

The histogram and cumulative distribution function of model error are depicted on figure 1.19. The maximum error of created model is -32.5dB and mean error reaches -56.5dB. In case of 90% of test samples the error is below -50dB and for 54% of samples the error is below -60dB.

1.5.3 Summary

In table 1.11 presented is a detailed comparison of described models. It can be seen, that the model accuracy strongly depends on complexity of the structure and number of variables.

Table 1.11: Comparison of created models

Structure	N	M	Space divisions	Δ_{max} [dB]	Δ_{mean} [dB]	Δ_{90} [dB]
Octagonal inductor	4	285	0	-55	-67.3	-63
Waveguide iris	4	460	2	-38.55	-55.97	-51
MCM-D Capacitor	6	2131	0	-32.5	-56.5	-50

1.6 Applications

The proposed technique is versatile and can be applied for construction of surrogate models of different kind of microwave structures. In fact, every structure that is described with scattering parameters and has a smooth response can be modelled. Therefore one can create models of

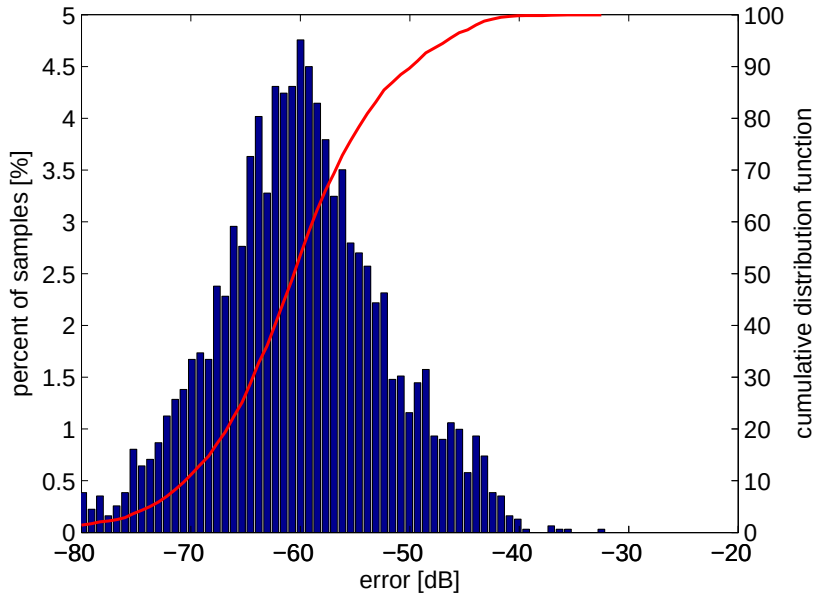

Figure 1.19: Histogram and cumulative distribution function of model error for interdigitated capacitor

elements made in various technologies: waveguide, microstrip, coplanar or multilayer. To show the benefits of models application two advanced examples are presented below.

1.6.1 Inductor optimization

High Q inductors is one of the problems in on-chip solutions for RF and microwaves.It is a common problem of designers to find an inductor that at frequency f realizes an inductance L_0 and in the same time minimize the inductor's area S and/or maximize the Q. It is an important issue, since there exist several designs of inductor with the same value of inductance L_0 and different values of quality factor and size. Several papers have investigated the inductor optimization problem [20, 21, 22, 23]. Authors propose to create a simple closed-form model of inductor parameters, like in [20, 23], but such models are difficult to find for multivariate case.

This problem can be solved using optimization procedure. Frequency dependent parameters of the inductor can be evaluated from its admittance parameters as [20]:

$$L(f,\underline{X}) = \frac{1}{2\pi f \cdot Im(Y_{11}(f))} \tag{1.13}$$

$$Q(f,\underline{X}) = -\frac{Im(Y_{11}(f))}{Re(Y_{11}(f))} \tag{1.14}$$

Both parameters L and Q of inductor depend of frequency f and dimensions of the structure $\underline{X} = [x_1\ x_2\ \ldots\ x_N]$. The procedure of inductor search can be organized as a simple optimization routine with goal function G defined as:

$$G(f_0,\underline{X}) = \|L(f_0,\underline{X}) - L_0\| - Q(f_0,\underline{X}) + \sum_{i=1}^{N} x_i \tag{1.15}$$

which has to be minimized over space of inductor geometric parameters. The minimum of the goal function gives the desired value of L for the smallest inductor and highest Q factor. Obviously such search is time consuming if electromagnetic simulator is involved to compute the inductor parameters. However, such search can be performed very fast using a multivariate surrogate model of the inductor. To prove this, a model of octagonal inductor described in section 1.5.1 was investigated and several optimizations were performed using the above goal function. A few examples of designed inductors are shown in table 1.12. The time of design in all cases is below 1 second. It is extremely fast comparing to electromagnetic approach since the EM-simulation of inductor response on single frequency takes a few minutes. It has to be noted that the model parameter space is continuous but a foundry production process assumes limited resolution. Therefore final dimensions have to be rounded to obey the process design rules.

Table 1.12: Results for an octagonal inductor design: requested parameters, obtained Q-factor, approximated inductor size and time of optimization (MATLAB)

Requested parameters	Q	Time [s]	Aprox. size
f_0 = 0.92GHz, L_0 = 2.2nH	10.4	0.52	375μ m $\times$ 375μ m
f_0 = 1.8GHz, L_0 = 1.4nH	12.9	0.49	208μ m $\times$ 208μ m
f_0 = 2.45GHz, L_0 = 2nH	16.8	0.7	236μ m $\times$ 236μ m
f_0 = 5.1GHz, L_0 = 1.1nH	17.7	0.45	172μ m $\times$ 172μ m

1.6.2 Waveguide filter

Surrogate models can be applied to design complex microwave components. For example, a 5-th order microwave filter with two dispersive stubs was divided into a separate discontinuities that have been modelled using the proposed approach, as presented in figure 1.20. In the same figure a comparison of the model response and the electromagnetic simulator is presented. In can be seen that model response is very accurate. What is important, it takes about 1 second to compute model response, which is much significantly faster comparing to over 2 minutes in case of electromagnetic analysis (mode-matching).

1.7 Problems with grid-based solvers

The most important issue for a successful creation of rational model based on the electromagnetic simulation is a smooth change of simulator response due to changes of structure geometry. It is a common feature of mode-matching based simulators, but may cause problems if a grid-based solvers (like MoM or FDTD) are used. The problem is illustrated in figure 1.21, where the S_{11} response of a microstrip stub on the MCM-D substrate versus width of the stub is presented. The structure is simulated at the frequency 1GHz and re-meshed each time the structure dimensions changes. Mesh frequency is also set as 1GHz. It can be seen that the transfer function is not smooth, which indicates non-physical response. A discontinuity of the response causes a huge problem for interpolation of data using rational functions.

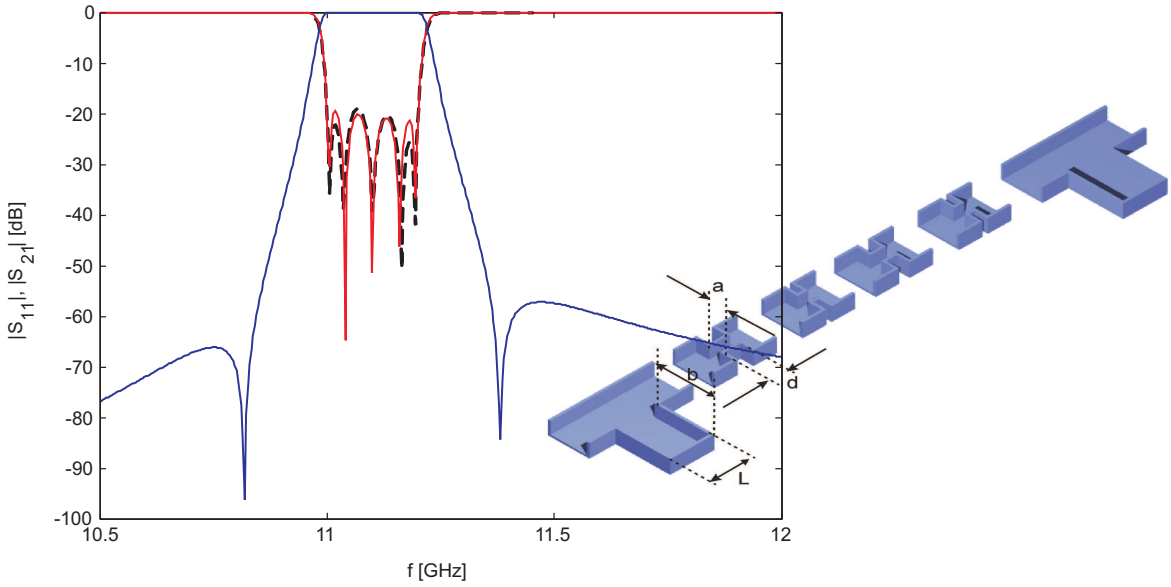

Figure 1.20: Waveguide filter structure and comparison of model response with results of electromagnetic simulator (mode-matching).

A way to circumvent this problem is to simulate the structure with a grid that is denser than the one resulting by considering the frequency alone. In the same figure the response of the same device is shown with mesh frequency set as 100GHz. In this case the response is smooth with change of the geometry. A drawback of such solution is an increased simulation time, due to denser mesh.

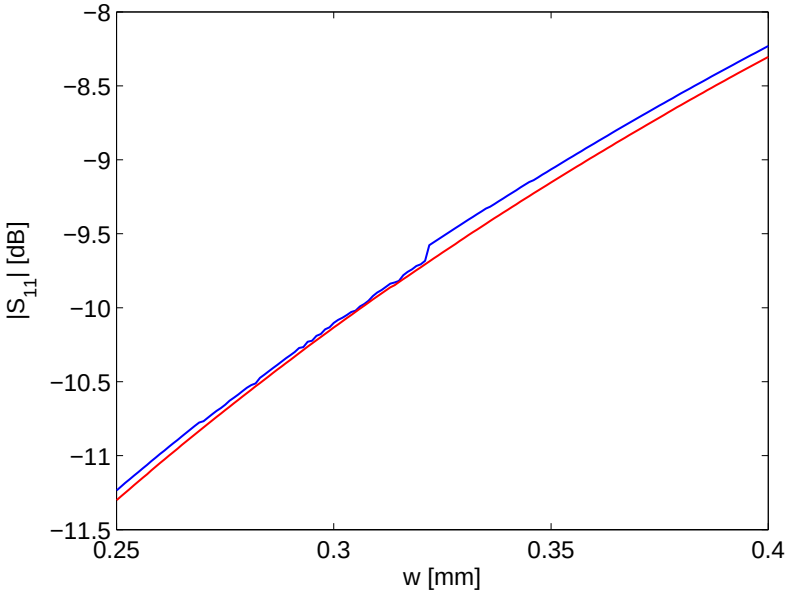

Figure 1.21: Response of the stub on the MCM-D substrate in function of stub width: — mesh computed at 1GHz, — mesh computed at 100GHz

Chapter 2

Integration with circuit simulators

The second goal of the grant was to integrate the developed techniques with the industry standard circuit simulators. Two issues are of importance:

- Generation of support points
- Integration of surrogate models with circuit simulators

2.1 Obtaining data from planar simulators

The algorithm of automatic model creation depends on the results of electromagnetic simulations. Because of continuity of parameter space and numerous support points, the algorithm must be able to create necessary structure, analyze it in a simulator and get the results. Most popular planar simulators can be used as a source of data samples, e.g. Sonnet, AWR Microwave Office or Agilent Momentum. Details of implementations will be explained taking as an example simple microstrip tee structure, simulated on single frequency point $2GHz$, shown on Fig.2.1. The substrate parameters are as follows: height $0.25mm$, dielectric constant 9.6, conductor conductivity $1 \cdot 10^{50} S$ without dielectric losses and enclosure without cover.

2.1.1 Sonnet simulator

Sonnet simulator can be run in a batch mode from command line taking as an input a text file containing all information needed for analysis. This is done by running a command:

```
em.exe input_file.son
```

Results of simulation, i.e. scattering parameters, are stored in file *log_response.log* in *son-data* subfolder. Simple text file parsing is sufficient to extract numeric data.

Because of the complexity of simulator and great number of options, only those relevant to modeling application are described in the next section. The input file format description is based on version 10.51 of Sonnet released in December 2004.

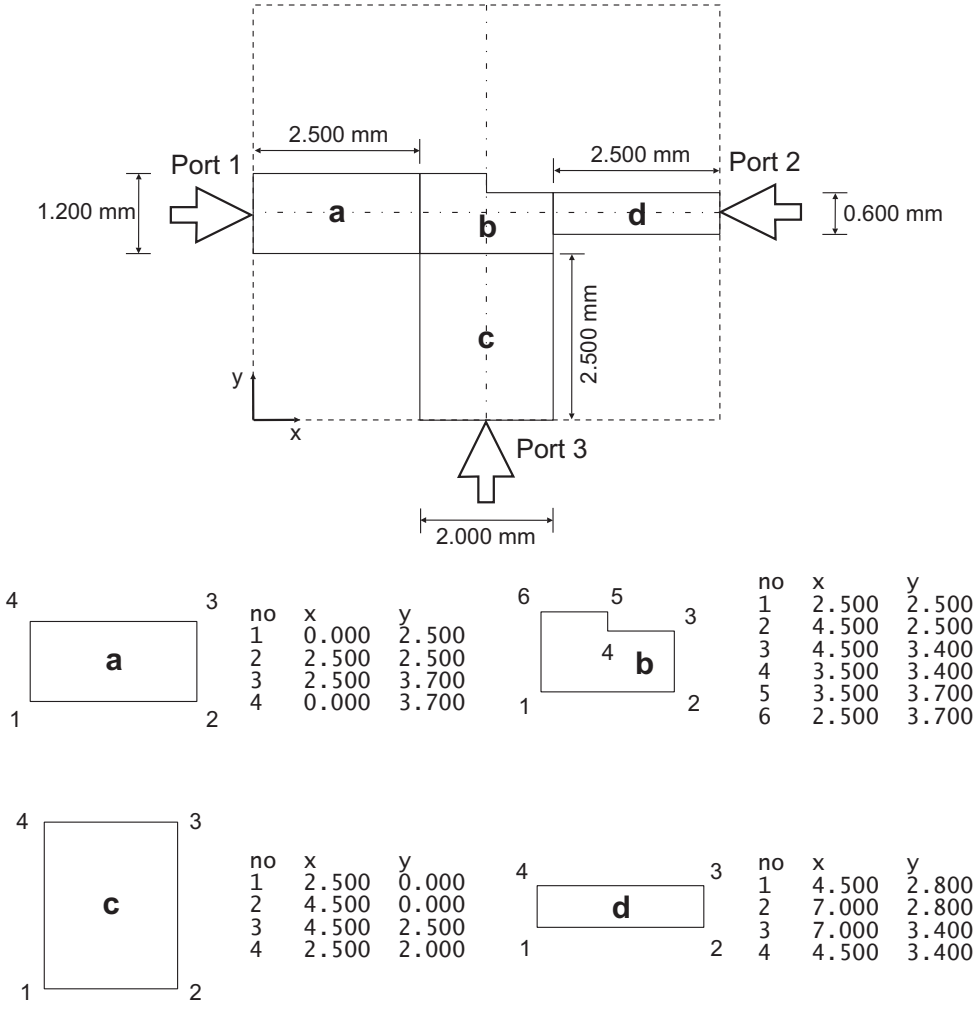

Figure 2.1: An example of microstrip tee structure.

Input file format

The first two lines of the input file contain only identification information irrelevant to simulation. For example, following two lines indicate a sonnet project file created in version 10.51 of the simulator.

```
FTYP SONPROJ 1 ! Sonnet Project File VER 10.51
```

The rest of the file is divided into following sections:

- HEADER
- DIM
- FREQ
- CONTROL
- GEO

Each section begins with ***section_name*** string and ends with **END *section_name*** string. For example:

```
HEADER ... END HEADER
```

HEADER section

The first section has a similar purpose as the first two lines of the file. It contains information not related to the simulation, e.g. information about license and dates of creation, modification of the project, and can be omitted during the input file generation for modeling. An example of this section looks as follows:

```
HEADER
    LIC SL00000.101
    DAT 04/11/2006 14:38:49
    BUILT_BY_CREATED xgeom 10.51 04/11/2006 14:25:39
    BUILT_BY_SAVED xgeom 10.51
    MDATE 04/11/2006 14:26:38
    HDATE 04/11/2006 14:26:02
END HEADER
```

DIM section

The DIM section must contain definitions of units of several dimensions. All numerical values in the input file must correspond to the units defined. Definition of every dimension unit takes one line a has a following format:

```
dim_id dim_unit
```

where **dim_id** is identification string of the dimension and **dim_unit** is a string indicating the unit. The table below shows all the dimension which definitions of units are needed.

Table 2.1: Description of dimension units.

Dimension	dim_id	dim_unit
Frequency	FREQ	Hz, KHz, MHz, GHz, THz, PHz
Inductance	IND	H, MH, UH, NH
Longitude	LHG	M, MM, UM, MIL, IN
Angle	ANG	DEG
Conductivity	CON	/OH
Capacitance	CAP	F, MF, UF, NF, PF
Resistance	RES	OH

An example of the DIM section is shown below:

```
DIM
    FREQ GHZ
    IND NH
    LNG MM
```

```
    ANG DEG
    CON /OH
    CAP PF
    RES OH
END DIM
```

FREQ section

Frequency points are defined in FREQ section. It is possible to define them in the same way as in GUI of the simulator. Thus frequency point can be defined as follows:

```
STEP freq_point
```

or

```
SIMPLE low_freq high_freq interval
```

where **freq_point** is a frequency of a single point, **low_freq** and **high_freq** are limits of a set of frequency points with **interval** between the points. For example the following line:

```
STEP 2.455
```

sets a frequency point at 2.455 units of frequency, and the next line:

```
SIMPLE 2.50 2.80 0.1
```

defines 31 frequency points from 2.50 to 2.80 units with an interval of 0.1 units. Other types of frequency points definition are irrelevant for modeling purposes.

CONTROL section

This section includes simulation options. The most important ones are:

```
SPEED value
```

where **value** indicates preset setting of mesh density influencing accuracy and speed of analysis. The **value** can be 0, 1 or 2. The lower the value is, the more accurate and slower simulation is. Another useful command in **CONTROL** section is:

```
OPTIONS -d
```

meaning that ports will be de-embedded from results.

GEO section

This section of the input file contains all information about geometry of the structure, including box, dielectric and metallization layers parameters. First, the top and the bottom metals must be defined. It can be chosen from three predefined types:

- Lossless, models a perfect conductor

  ```
  TMET "Lossless" 0 SUP 0 0 0 0
  ```

- Load, models a perfect matched waveguide load

  ```
  TMET "WG Load" 0 WGLOAD
  ```

- Free Space, which removes the top or bottom cover

```
TMET "Free Space" 0 FREESPACE 376.7303136 0 0 0
```

It is also possible to set a user-defined metal as the top or the bottom metal. For the top metallization it can be done placing following line:

```
TMET "metal_name" metal_no NOR metal_cond metal_cr metal_thick
```

where **metal_name** is a unique name of the metal, **metal_no** is a successive number of the metal, i.e. 1 for the first user-defined metal, **metal_cond** is the metal conductivity, **metal_cr** is the current ratio and **metal_thick** is the thickness of the metal.

It is required that user-defined metal must be declared in a separate line in the same way as **TMET** but with **MET** command, for example:

```
MET "Metal2" 1 NOR 1000 0 0.01
```

If a circuit is symmetric about the center line parallel to the X axis, then the symmetry can be activated by placing the following line:

```
SYM
```

which results in faster analysis.

Specification of the box containing the structure consists of a line defining box dimensions and lines containing dielectric layers information. The box dimensions are defined as:

```
BOX met_lay_no box_x box_y cells_x cells_y 20 0
```

where **met_lay_no** is a number of metallization layers, **box_x** and **box_y** are dimensions of the box, **cells_x** and **cells_y** are twice the numbers of cells horizontally and vertically respectively. For example the following line:

```
BOX 4 320 320 256 256 20 0
```

defines a box with four layers of metallization (five dielectric layers) with dimensions 320x320 units divided on 128 cells horizontally and vertically.

Each dielectric layer must be defined in a separate line of the form:

```
d_thick d_const m_perm d_loss m_loss d_cond 0 "d_name"
```

where **d_thick** is the thickness of the layer, **d_const** is the dielectric constant, **m_perm** is the relative magnetic permeability, **d_loss** is the dielectric loss tangent, **m_loss** is the magnetic loss tangent, **d_cond** is the dielectric conductivity and **d_name** is a unique name of the layer. For example the following line:

```
25 12.9 1 0 0 0 2 "GaAs"
```

defines a lossless layer of gallium arsenide 25 units thick.

Definition of ports spans over four lines. The first line begins port declaration:

```
POR1 port_type
```

where **port_type** can be **STD** for a standard port or **AGND** for an autogrounded port. The second line binds the port with a specific polygon of metallization:

```
POLY poly_id 1
```

where **poly_id** is a unique number of the polygon to which the port is adjacent.. The third line defines an edge the box the port is adjacent to. For example:

```
3
```

means that the port is adjacent to left edge of the box. The other values are: 0 for top edge, 1 for right edge and 2 for bottom edge. The last line of port declaration declares the number of the port, the port impedance and its position:

```
port_no port_res port_react port_ind port_cap port_x port_y
```

where **port_no** is a successive number of the port, **port_res** and **port_react** are real and imaginary parts of the port impedance, **port_ind**, **port_cap** are inductance and capacitance of the port and **port_x** and **port_y** are coordinates of the port. For example the following line:

```
2 50 0 0 0 320 160
```

defines a second port with purely resistive impedance of 50 units at position x=320 and y=160.

Reference planes can be moved away from the edge of the box by placing a line:

```
DRP1 rp_pos FIX rp_dist
```

where **rp_pos** indicates the edge of the box of reference plane displacement (can be **LEFT**, **RIGHT**, **TOP** or **BOTTOM**), **rp_dist** is a distance of the reference plane from the specified edge. For example, the following line:

```
DRP1 RIGHT FIX 1.20
```

sets reference place for ports on the right edge at a distance of 1.20 units from the edge.

Shapes of metallization or dielectric are drawn in a form of polygons. Description of a polygons begins with a line indicating the total number of polygons in the structure. For example:

```
NUM 2
```

indicates there are two polygons to be defined below. Declaration of a single polygon begins with the following line:

```
layer_no poly_vert metal_no N poly_id sub_xmin sub_ymin sub_xmax
sub_ymax 0 0 0 egde_mesh
```

where **layer_no** is a metallization layer number, **poly_vert** is a number of vertices in the polygon (including a duplicate vertex at the end of the list), **metal_no** is metal number (equivalent to metal number in user-defined metals), **poly_id** is an unique polygon id, **sub_xmin**, **sub_ymin**, **sub_xmax** and **sub_ymax** are subsectioning controls, **egde_mesh** turns on/off edge mesh and can be either **Y** or **N**.

Dimensions of the polygon are specified by defining the position of all vertexes in the polygon. The position of each vertex is described by the line:

```
poly_x poly_y
```

where **poly_x** and **poly_y** are positions relative to a coordinate system of the structure. Note that the last vertex must be the same as the first one.

For example block below:

```
0 5 -1 N 12 1 1 100 100 0 0 0 Y 320 147.5 320 172.5 220 172.5 220
147.5 320 147.5 END
```

defines a rectangle in the first metallization layer with id 12 with dimensions 100x25 units and bottom left corner at the position x=220 and y=147.5 units.

Example

The structure presented on Fig.2.1 would be described by a file which most important sections are:

- FREQ section for a single frequency point at $2GHz$

  ```
  FREQ
  SIMPLE 2.0
  END FREQ
  ```

- GEO section with box and dielectric layers parameters

  ```
  GEO
  TMET "Free Space" 0 FREESPACE 376.7303136 0 0 0
  BMET "Lossless" 0 SUP 0 0 0 0
  BOX 1 7 6.2 140 124 20 0
        30 1 1 0 0 0 0 "Air"
        0.25 9.6 1 0 0 1e+050 0 "substrate"
  ```

  ... ports definitions ...

  ```
  POR1 STD
  POLY 1002 1
  3
  1 50 0 0 0 0 3.1
  POR1 STD
  POLY 1003 1
  2
  3 50 0 0 0 3.5 6.2
  POR1 STD
  POLY 1005 1
  1
  2 50 0 0 0 7 3.1
  ```

  ... and metallization polygons

```
NUM 4
0 5 -1 N 1002 1 1 100 100 0 0 0 Y
0 2.5
2.5 2.5
2.5 3.7
0 3.7
0 2.5
END
0 5 -1 N 1003 1 1 100 100 0 0 0 Y
2.5 3.7
4.5 3.7
4.5 6.2
2.5 6.2
2.5 3.7
END
0 5 -1 N 1005 1 1 100 100 0 0 0 Y
4.5 2.8
7 2.8
7 3.4
4.5 3.4
4.5 2.8
END
0 7 -1 N 1006 1 1 100 100 0 0 0 Y
2.5 3.7
2.5 2.5
3.5 2.5
3.5 2.8
4.5 2.8
4.5 3.7
2.5 3.7
END
END GEO
```

2.1.2 AWR Microwave Office

Microwave Office implements a COM-compatible interface allowing easy communication with other software. All functions related to creating EM structures within simulator's GUI have COM counterparts. Thus creating the structure is straightforward and consists of the following steps presented in pseudocode taking as an example the structure from Fig. 2.1:

1. Starting new project

   ```
   proj = MWO.New( 'eoard' )
   ```

2. Creating an empty EM structure

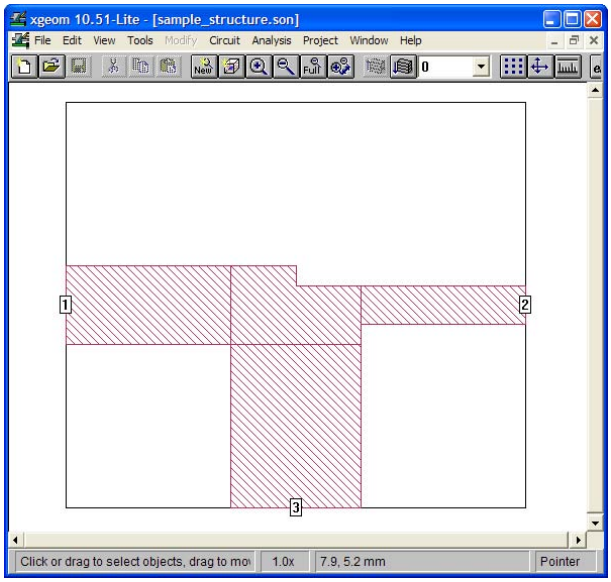

Figure 2.2: View of the example structure in Sonnet window.

```
emstructure = proj.EMStructures.Add( 'mstrip tee' )
```

3. Setting substrate - when creating the EM structure, there are two default material layers. Thus no new layers must be created in this case - only the existing ones need to be modified. For setting the substrate parameters:

```
layer2 = MaterialLayers.Item(2)
layer2.Thickness = 0.25
layer2.DielectricConstant = 9.6
layer2.LossTangent = 0.0
```

and for the air layer:

```
layer1 = MaterialLayers.Item(1)
layer1.Thickness = 4.0
layer1.DielectricConstant = 1.0
layer1.LossTangent = 0.0
```

Setting the enclosure requires the following commands:

```
emstructure.Enclosure.XDimension = 0.0070
emstructure.Enclosure.YDimension = 0.0062
emstructure.Enclosure.XDivisions = 70
emstructure.Enclosure.YDivisions = 62
```

```
emstructure.Enclosure.Height     = 4.0
emstructure.Enclosure.EnclosureTop = mwBMT_ApproximateOpen
```

4. Drawing metallization shapes

```
emstructure.Shapes.AddRectangle( 0, 0.0025, 0.0025, 0.0012 )
emstructure.Shapes.AddPolygon( [ 0.0010 0.0025;
                                 0.0025 0.0020;
                                 0.0045 0.0025;
                                 0.0030 0.0045;
                                 0.0034 0.0040;
                                 0.0035 0.0034;
                                 0.0050 0.0035;
                                 0.0037 0.0060;
                                 0.0025 0.0037 ] )
emstructure.Shapes.AddRectangle( 0.0025, 0, 0.0020, 0.0025 )
emstructure.Shapes.AddRectangle( 0.0045, 0.0028, 0.0025, 0.0006 )
```

5. Adding ports

```
emstructure.Shapes.AddPort( 0.0000, 0.0025, 0.0000, 0.0031, 1 )
emstructure.Shapes.AddPort( 0.0070, 0.0028, 0.0070, 0.0034, 1 )
emstructure.Shapes.AddPort( 0.0025, 0.0000, 0.0045, 0.0000, 1 )
```

6. Setting frequency of simulation

```
proj.Frequencies.Add( 2.000 )
```

7. Launching simulation

```
proj.Simulate()
```

8. Obtaining simulation results - adding a graph:

```
graph = proj.Graphs.Add( 'mstrip tee s-parameters', 4 )
```

setting its parameters:

```
mes = graph.Measurements.Add( 'mstrip tee', 'Re(S(1,1))' )
mes = graph.Measurements.Add( 'mstrip tee', 'Im(S(1,1))' )
```

and getting results

```
result = mes.YValues;
```

Detailed description of Microwave Office API can be found in [24].

2.1.3 ADS Momentum

Generation of a structure in Momentum is not as straightforward as in Sonnet or Microwave Office because of numerous files generated by Momentum engine. Even so shapes of metallization, stored in *proj.* file, and substrate information, stored in *proj.sub*, are simple text files.

Example

The ports and metallization shapes are defined in *proj.* file:

```
UNITS MM,10000;
ADD N1 :F1.0 :S0 :T1003 :D '1, 50, 0, 0' 0, 3.1;
ADD N1 :F1.0 :S0 :T1003 :D '2, 50, 0, 0' 7, 3.1;
ADD N1 :F1.0 :S0 :T1003 :D '3, 50, 0, 0' 3.5, 0;
ADD P1
 0.000000,3.700000
 2.500000,3.700000
 2.500000,2.500000
 0.000000,2.500000
 0.000000,3.700000;
ADD P1
 2.500000,2.500000
 4.500000,2.500000
 4.500000,0.000000
 2.500000,0.000000
 2.500000,2.500000;
ADD P1
 4.500000,3.400000
 7.000000,3.400000
 7.000000,2.800000
 4.500000,2.800000
 4.500000,3.400000;
ADD P1
 3.500000,3.400000
 4.500000,3.400000
 4.500000,2.800000
 4.500000,2.500000
 2.500000,2.500000
 2.500000,3.700000
 3.500000,3.700000
 3.500000,3.400000;
```

The box and dielectric layers are described in *proj.sub* file:

```
UNITS METRE
BOTTOMPLANE IMPEDANCE 0 0
TOPPLANE OPEN

LAYERS
0 THICKNESS INFINITY
  PERMITTIVITY VALUE 1 0
  PERMEABILITY VALUE 1 0
,
1 THICKNESS 0.00025
  PERMITTIVITY VALUE 9.6 0
  PERMEABILITY VALUE 1 0
  STRIP
;
```

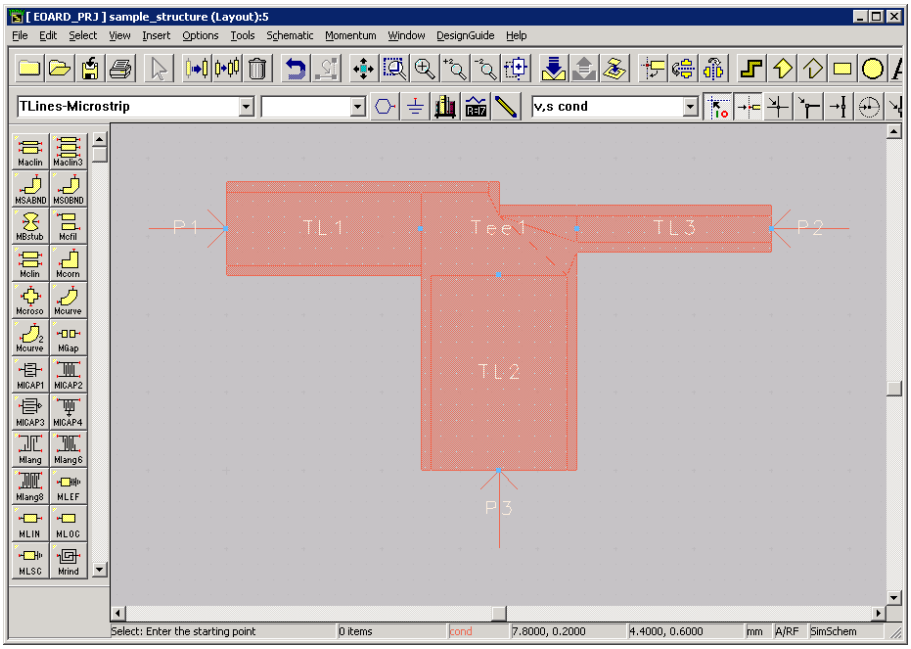

Figure 2.3: View of the example structure in ADS Momentum window.

2.2 Integration with circuit simulators

Surrogate models created using the presented technique can be incorporated into industry standard circuit simulators like Agilent's Advanced Design System or AWR's Microwave Office.

2.2.1 ADS Schematic

Advanced Design System allows one to create user-defined models using one of the following method:

1. Model Composer
2. Advanced Model Composer
3. User-Compiled Model

Model Composer and Advanced Model Composer create automatically models of layout elements that can be used in linear simulations. They use polynomial interpolation with reflective exploration technique. Elements that can be modeled using Model Composer are limited to a set of typical microstrip discontinuities, e.g. bends, corners, crosses or gaps on a single non-parameterized substrate. The substrate can be parameterized in Advanced Model Composer, but for both techniques recommended number of continues parameters is two, thus limiting modeled elements to very simple ones.

User-Compiled Model function does not create any models itself, but allows incorporating user-coded models of any layout element and potentially removing the limitations of the number of parameters. Linear user-compiled models can have up to 99 external ports but there is no hard-coded limitation regarding number of parameters. The making of a model consists of three steps:

1. Defining the parameters whose values will be entered from the schematic
2. Defining the symbol and the number of pins
3. Writing the C-code

Definition of the parameters of the model consists of declaring parameter's name, description, default value and type. Validation of parameter's range must be implemented by the user.

The C-code must return Y matrix of the element provided with element parameters. User-Compiled Model function automatically creates a template code with a header file for necessary procedures that must be complemented by a user code. Although the code must conform to ANSI-C standard, C++ compiler is needed for linking the entire program.

Implementation details

Details of model implementation in ADS are presented taking as an example the MCM-D capacitor model. The first step is the definition of model parameters depicted on Fig.2.4. For every parameter its name, default value and type are defined.

The next step is to draw schematic symbol for the model (Fig.2.5) where the number of pins defines number of ports of the model.

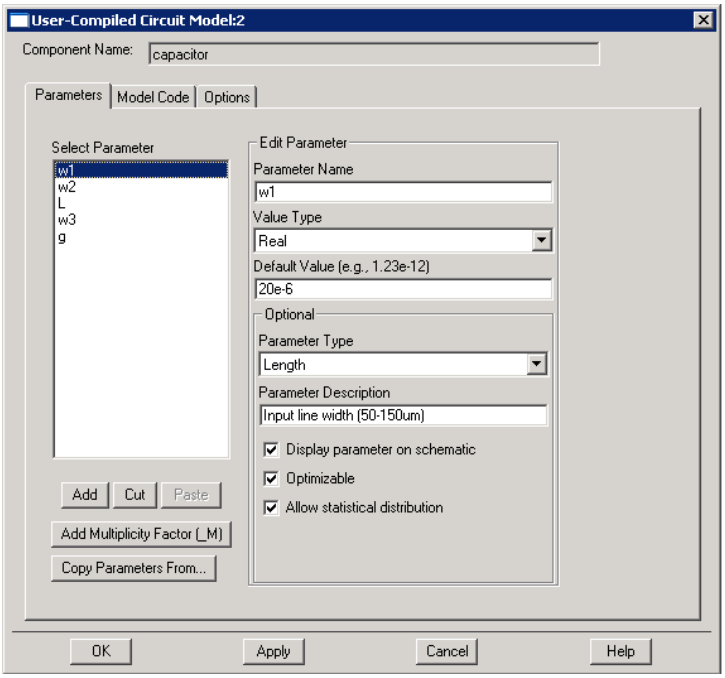

Figure 2.4: Parameters editor window.

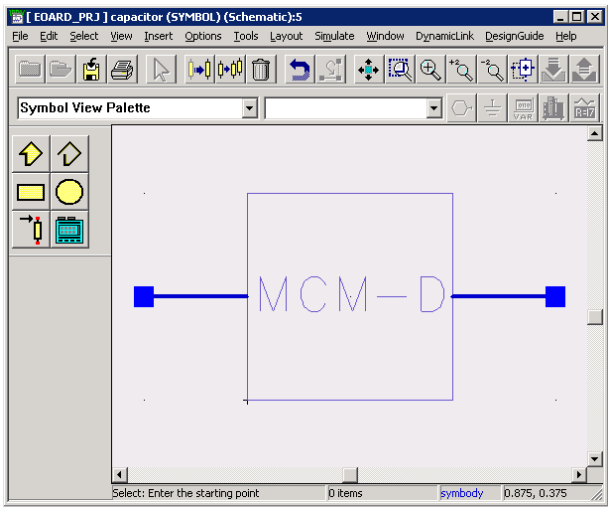

Figure 2.5: View of schematic window when editing model symbol.

The main step is writing the C-code for the model calculating its Y-parameters. A diagram of rational model implementation is depicted on Fig.2.6, where the main part of the implementation is a function:

```
boolean compute_y(UserInstDef *userInst, double omega, COMPLEX *yPar)
```

The parameters typed in a schematic window are passed into the function in an array

`userInst->pData[]`

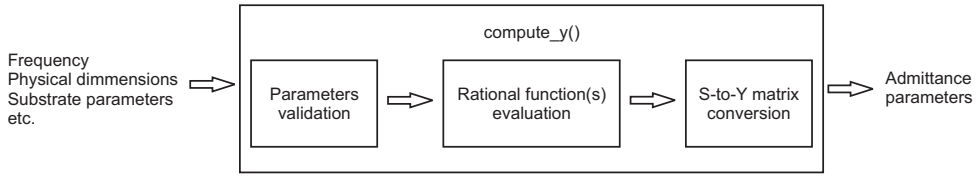

Figure 2.6: Diagram of model implementation in Agilent's ADS.

and are easily accessible through macros defined in the header file. Frequency of simulation is passed in *omega* parameter. The *yPar* parameter is a pointer to an array of complex admittance parameters that the function must return. Note that COMPLEX type is not present in ANSI-C standard. It is defined as a struct:

```
typedef struct {
  double real;
  double imag;
} COMPLEX;
```

and thus all mathematical operations on COMPLEX type variables must be implemented by the user. Because the model describes S-parameters of the capacitor, the scattering matrix must be converted to the admittance matrix prior return statement. The conversion is done by the function provided by ADS:

```
extern boolean s_y_convert(COMPLEX *inPar, COMPLEX *outPar, int direction, double rNo
```

taking as the parameters, besides input and output matrices, direction of conversion (i.e. S-to-Y or Y-to-S), reference impedance and the number of ports of the model. Complete listing of the *compute_y* function of MCM-D capacitor model is presented below.

```
static boolean compute_y(
  UserInstDef *userInst,
  double omega,
  COMPLEX *yPar)
{
    boolean status = TRUE;
    COMPLEX Smatrix[4];
    double f;       // frequency
    double x[6];    // vector of parameters

    f = omega/2/PI; // conversion to Hz

    // populating 'getmodelSXX' input vector
    x[0] = f/1e9;
    /*
        g_P is a macro:
        #define G_P  userInst->pData[0].value.dVal
        which is gap width parameter in milimeters
    */
```

```
    x[1] = 1e3*g_P;
    x[2] = 1e3*w3_P;
    x[3] = 1e3*L_P;
    x[4] = 1e3*w2_P;
    x[5] = 1e3*w1_P;

    /*
        Function:
        COMPLEX getmodelS11( int n, double* x )
        return s11 parameter of the model, where
        x is a vector of parameters in meters and Hz
    */
    Smatrix[0] = Smatrix[3] = getmodelS11( 1, &x[0] );
    Smatrix[1] = Smatrix[2] = getmodelS21( 1, &x[0] );

    s_y_convert( Smatrix, yPar, 1, Z0, 2);

    return status;
}
```

After compiling written code in User-Compiled Model window the model is accessible in Component Library in schematic window (Fig.2.7).

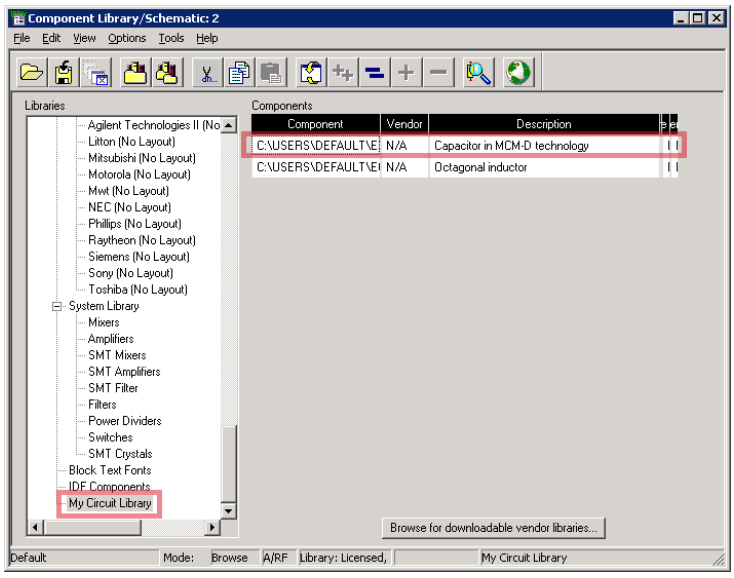

Figure 2.7: View of Component Library window in schematic showing user-compiled models.

The model can be placed into schematic window in the same way as built-in models and used in linear simulation, as shown on Fig.2.8.The results of simulation of the circuit in schematic as well as in Momentum (Fig.2.10) are shown on Fig.2.9.

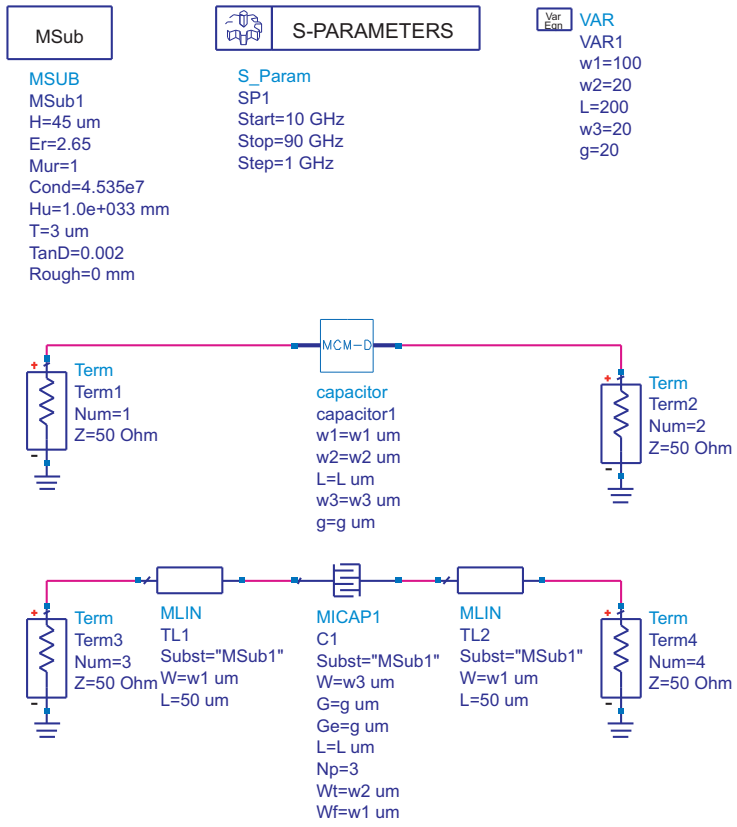

Figure 2.8: View of schematic window with implemented MCM-D capacitor model and ADS intergidital capacitor model.

a) b)

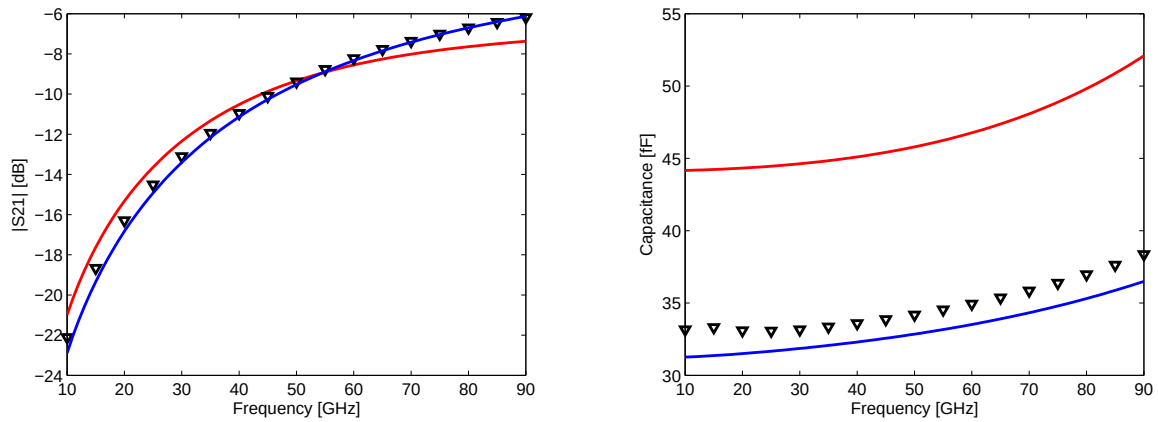

Figure 2.9: Results of simulations of the example of MCM-D capacitor. The red line represents ADS interdigital capacitor model, blue line represents rational model, black triangles are the results of Momentum simulations.

2.2.2 AWR Microwave Office

Custom models in Microwave Office can be created using Model Wizard from Software Development Kit. The modeling wizard generates a C++ description of the model that can be

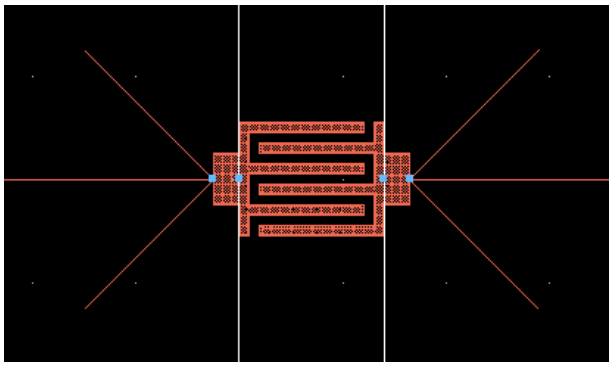

Figure 2.10: Layout of MCM-D capacitor in Momentum.

compiled as a dynamically linked model. The models are implemented using Microsofts COM (Component Object Model) technology used for communication between different software in Windows family operating systems. Conformity to COM standard allows easy migration to future versions of Microwave Wizard without recompiling any binaries. One can add the model just by placing compiled file into ”Models” subfolder of the simulator folder. Steps needed to create a model are as follows:

1. Code generation
2. Model implementation
3. Compilation

Similarly to Agilent’s simulator, most of the source code is generated by the simulator, precisely by the Model Wizard (see Fig.**??**). The implementation of the code is analogous to ADS models and is limited to writing the mathematical description of the model between following lines of comments:

```
//[-USER CODE BEGIN-]
...
//[-USER CODE END-]
```

Compilation can be done using C++ compiler linking user-modified .cpp file with the Compiler Dependent Library. Multiple *.cpp files can be batch compiled so that multiple models can be implemented within a single dll.

Implementation details

```
KCmplxMtxData Smat(2,2);
double x[6];
x[0] = freq/1e9;
x[1] = g/1e-3;
x[2] = w3/1e-3;
x[3] = L/1e-3;
x[4] = w2/1e-3;
```

```
x[5] = w1/1e-3;

Smat(1,1) = Smat(2,2) = getmodelS11( 1, &x[0] );
Smat(1,2) = Smat(2,1) = getmodelS21( 1, &x[0] );

AWR_Smat2Ymat( Smat, 2, NULL, ymat );
```

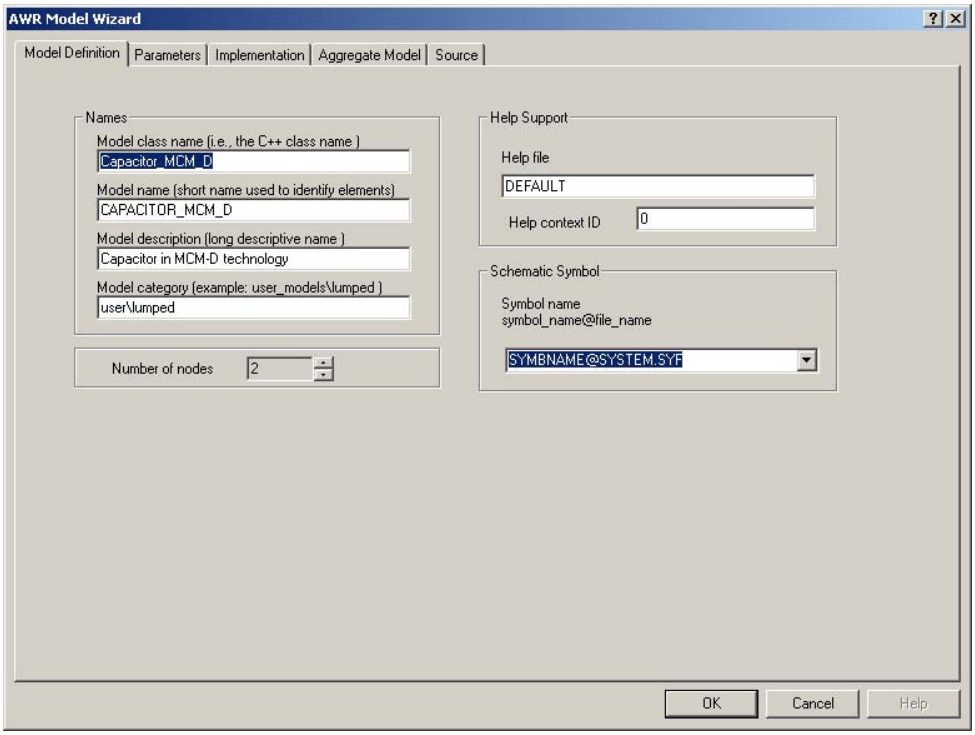

Figure 2.11: Model Wizard in Microwave Office.

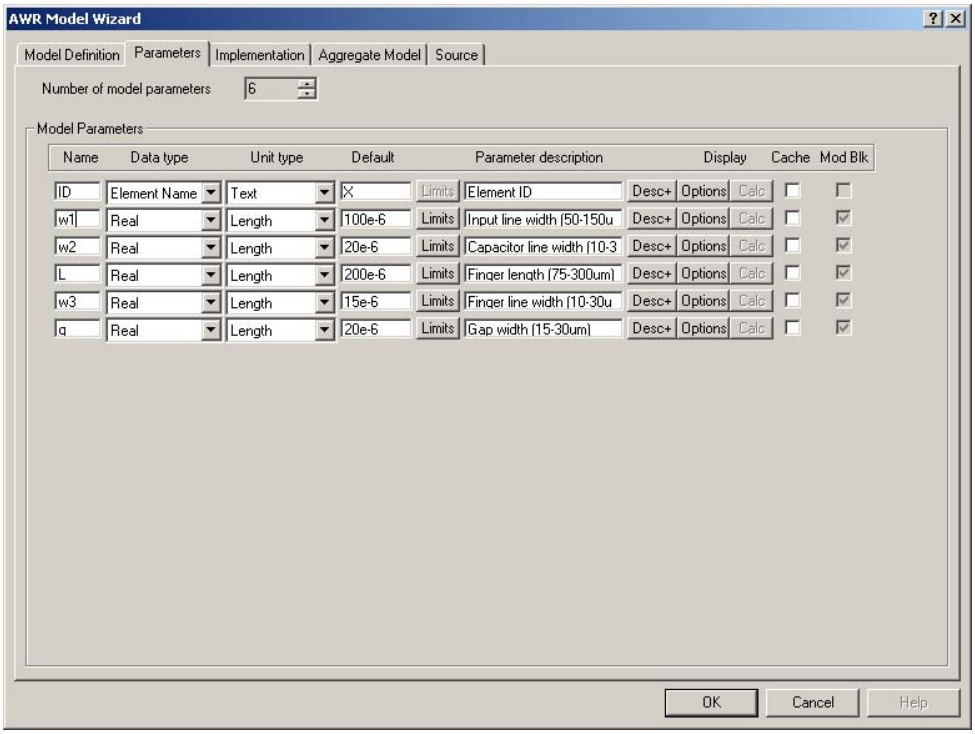

Figure 2.12: Parameter editor in the Model Wizard.

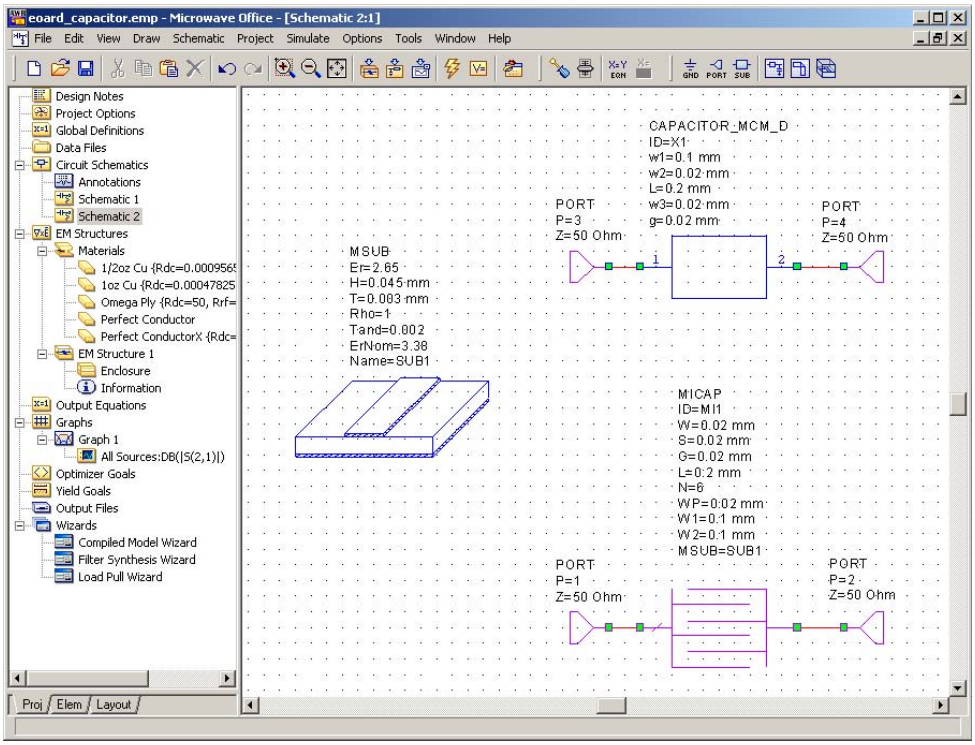

Figure 2.13: Model Wizard in Microwave Office.

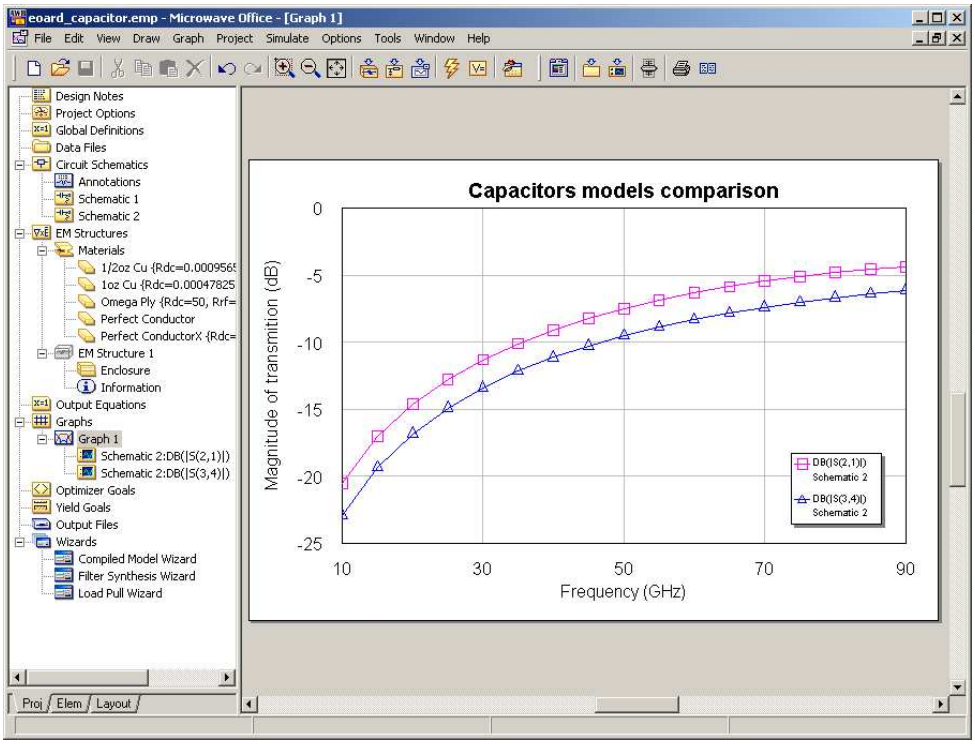

Figure 2.14: Model Wizard in Microwave Office.

Bibliography

[1] A. Lamecki, P. Kozakowski, and M. Mrozowski. Efficient implementation of the cauchy method for automated cad-model construction. *IEEE Microwave and Wireless Components Letters*, 13:268–270, July 2003.

[2] A. Lamecki, P.Kozakowski, and M. Mrozowski. Multimode, multiparametric surrogate models for fast design of waveguide components. In *European Microwave Conference*, Munich, Germany, October 2003.

[3] A. H. Zaabab, Q. J. Zhang, and M. Nakhla. A neural network modeling approach to circuit optimization and statistical design. *IEEE Transactions on Microwave Theory and Techniques*, 43:1349–1558, June 1995.

[4] V. K. Devabhaktuni, M. C. E. Yagoub, and Qi-Jun Zhang. A robust algorithm for automatic development of neural-network models for microwave applications. *IEEE Transactions on Microwave Theory and Techniques*, 49:2282–2291, December 2001.

[5] G. L. Creech, B. J. Paul, C. D. Lesniak, T. J. Jenkins, and M. C. Calcatera. Artificial neural networks for fast and accurate em-cad of microwave circuits. *IEEE Transactions on Microwave Theory and Techniques*, 45:794–801, May 1997.

[6] T. A. Driscoll and B. Fornberg. Interpolation in the limit of increasingly flat radial basis functions. *Computers and Mathematics with Applications*, 43:413–422, 2002.

[7] A. Lamecki and M. Mrozowski. Cad-model construction based on adaptive radial basis functions interpolation technique. In *15-th International Conference on Microwaves, Radar and Wireless Communications Mikon*, Warszawa, May 2004.

[8] S. Rippa. An algorithm for selecting a good value for the parameter c in radial basis function interpolation. *Advances in Computational Mathematics*, 11:193–210, 1999.

[9] J. De Geest, T. Dhaene, N. Fache, and D. De Zutter. Adaptive cad-model building algorithm for general planar microwave structures. *IEEE Transactions on Microwave Theory and Techniques*, 47:1801–1809, September 1999.

[10] P. Meyer R. Lehmensiek. Creating accurate multivariate rational interpolation models of microwave circuits by using efficient adaptive sampling to minimize the number of computational electromagnetic analyses. *IEEE Transactions on Microwave Theory and Techniques*, 49:1419–1430, August 2001.

[11] P. Meyer R. Lehmensiek. Adaptive sampling applied to multivariate, multiple output rational interpolation models with application to microwave circuits. *Int Journal RF and Microwave*, 2002.

[12] R. Lehmensiek and P. Meyer. Using efficient multivariate adaptive sampling by minimizing the number of computational electromagnetic analysis needed to establish accurate interpolation models. In *IEEE MTT-S Internatial Microwave Symposium Digest*, USA, 2001.

[13] E. S. Siah, M. Sasena, J. L. Volakis, P. Y. Papalambros, and R. W. Wiese. Fast parameter optimization of large-scale electromagnetic objects using direct with kriging metamodeling. *IEEE Transactions on Microwave Theory and Techniques*, 52, January 2004.

[14] D. Staiculescu, J. Laskar, and E. M. Tentzeris. Design rule development for microwave flip-chip applications. *IEEE Transactions on Microwave Theory and Techniques*, 48, September 2000.

[15] R. S. Adve, T. K. Sarkar, S. M. Rao, E. K. Miller, and D. R. Pflug. Application of the cauchy method for extrapolating/interpolating narrow-band system responses. *IEEE Transactions on Microwave Theory and Techniques*, 45:837–845, May 1997.

[16] L. Balewski and M. Mrozowski. Evaluation of accuracy of surrogate models. In *16th International Conference on Microwaves, Radar and Wireless Communications*, 2006.

[17] R. H. Bartels and J. J. Jezioranski. Least-squares fitting using orthogonal multinomials. *ACM Transactions on Mathematical Software*, 11, September 1985.

[18] R. S. Adve, T. K. Sarkar, S. M. Rao, E. K. Miller, and D. R. Pflug. Application of the cauchy method for extrapolating/interpolating narrow-band system responses. *IEEE Transactions on Microwave Theory and Techniques*, 45:837–845, May 1997.

[19] G. H. Golub and Ch. F. Van Loan. *Matrix Computation*. The Johns Hopkins University Press, 1996.

[20] Ch. B. Sia, B. H. Ong, K. W. Chan, K. S. Yeo, J.-G. Ma, and M. A. Do. Physical layout design optimization of integrated spiral inductors for silicon-based rfic applications. *IEEE Transactions on Electron Devices*, 52, December 2005.

[21] S. Mukherjee, B. Mutnury, S. Dalmia, and M. Swaminathan. Layout-level synthesis of rf inductors and filters in lcp substrates for wi-fi applications. *IEEE Transactions on Microwave Theory and Techniques*, 53, June 2005.

[22] J. M. Lopez-Villegas, J. Samitier, Ch. Cane, P. Losantos, and J. Bausells. Improvement of the quality factor of rf integrated inductors by layout optimization. *IEEE Transactions on Microwave Theory and Techniques*, 48, January 2000.

[23] Ch. Zhen and G. Lihui. Application of the genetic algorithm in modeling rf on-chip inductors. *IEEE Transactions on Microwave Theory and Techniques*, 51, February 2003.

[24] *Microwave Office API Documentation, http://appwave.com/APIdocs*.